Development of a Drug-Eluting 3D Bioprinted Mesh (GlioMesh) for Treatment of Glioblastoma Multiforme

by

Reihaneh Hosseinzadeh
Bachelor of Science, Islamic Azad University of Shiraz, 2015

A Thesis Submitted in Partial Fulfilment
of the Requirements for the Degree of

MASTER OF APPLIED SCIENCE

in the Department of Mechanical Engineering

Supervisory Committee

Development of a Drug-Eluting 3D Bioprinted Mesh (GlioMesh) for Treatment of Glioblastoma Multiforme

by

Reihaneh Hosseinzadeh
Bachelor of Science, Islamic Azad University of Shiraz, 2015

Supervisory Committee

Dr. Mohsen Akbari, Department of Mechanical Engineering
Supervisor

Dr. Stephanie Willerth, Department of Mechanical Engineering
Departmental Member

Abstract

Supervisory Committee
Dr. Mohsen Akbari, Department of Mechanical Engineering
Supervisor
Dr. Stephanie Willerth, Department of Mechanical Engineering
Departmental Member

Glioblastoma multiforme (GBM) is among the most aggressive and mortal cancers of the central nervous system. Maximal safe surgical resection, followed by radiotherapy accompanied with chemotherapy is the standard of care for GBM patients. Despite this intensive treatment with conventional approaches, the management of GBM remains poor. The infiltrative nature of cancer cells makes the complete tumour removal by surgery virtually impossible. In addition, the blood-brain barrier's (BBB) lack of permeability limits the number of effective chemotherapy drugs for GBM. Temozolomide (TMZ) is the most widely used chemotherapeutic agent for GBM because of its ability to pass the BBB. However, high systemic doses required to achieve brain therapeutic level, resulting in numerous side effects. The recurrence of GBM is almost inevitable due to the aforementioned shortcomings of conventional methods of treatment. Therefore, a great deal of effort has been focused on the development of new treatment methods capable of providing a high concentration of chemotherapy drug at the tumour site. Microspheres made from biodegradable polymers hold great potential to keep the chemotherapeutic agent intact within the carrier and locally deliver the drug over an extended period. However, the encapsulation of amphiphilic drug molecules such as TMZ within poly (d, l-lactide-co-glycolide) (PLGA) microspheres with conventional emulsion methods, oil-in-water (o/w), water-in-oil-in-water (w/o/w), is a major challenge. The extremely low encapsulation efficiencies obtained for TMZ-loaded PLGA microspheres using the aforementioned

techniques (<7%) hampers the ability to scale up this process. Additionally, the injected microspheres to the tumour site tend to dislocate due to the cerebral flow which reduces the effectiveness of this localized drug delivery strategy. This study has focused on the development of a 3D bioprinted hydrogel-based mesh containing TMZ-loaded PLGA microspheres with high encapsulation efficiency (GlioMesh). To accomplish this, oil-in-oil (o/o) emulsion solvent evaporation technique was used to prepare PLGA microspheres loaded with TMZ. The poor solubility of TMZ in the external oil phase, liquid paraffin, resulted in obtaining encapsulation efficiencies as high as 61%. We then used the 3D bioprinting technology to embed TMZ-loaded PLGA microspheres into an alginate mesh. This provides the advantage of immobilizing the microspheres at the tumour site. Additionally, the flexibility and porosity of 3D bioprinted mesh allow for easy implantation and nutrients transportation to the brain tissue. The incorporation of polymeric microspheres within alginate fibres led to achieving an extended release of TMZ over 50 days. The functionality of GlioMesh in inducing cell cytotoxicity was evaluated by performing *in vitro* cell viability tests on U87 human glioblastoma cells. Higher cytotoxic effects were observed in the case of treatment with GlioMesh compared to the free drug because of the sustained release properties of our mesh. These data suggest that GlioMesh holds great promise to be used as an implant in the treatment of GBM.

Table of Contents

List of Tables

List of Figures

List of Abbreviation

Apo E - Apolipoprotein E

BBB - Blood-brain barrier

BCNU - 1,3-Bis(2-chloroethyl)-1-nitrosourea

BSA - Bovine serum albumin

CED - Convection-enhanced delivery

CT - Computed tomography

CAD - Computer-aided-design

DW - Diffusion-weighted

DPBS - Dulbecco's phosphate buffered saline

DMEM - Dulbecco’s modified Eagle medium

EE - Encapsulation efficiency

EGFR - Epidermal growth factor receptor

FBS - Fetal bovine serum

GBM - Glioblastoma multiforme

LDLR - Low-density lipoprotein receptors

MRI - Magnetic resonance imaging

MTIC - Monomethyl triazene 5-(3-methyltriazen-1-yl)-imidazole-4-carboxamide

O/o - Oil-in-oil

O/w - Oil-in-water

P16INK4a - P16 cyclin-dependent kinase inhibitor 4a

PTEN - Phosphatase and tensin homolog

PBCA - Poly (butyl cyanoacrylate)

PLGA - Poly (d, l-lactide-co-glycolide)

PEG - Poly (ethylene glycol)

PLA - Poly (lactic acid)

PCPP-SA - Poly-[bis-p-(carboxyphenoxy)propane-sebacic acid]

PVA - Polyvinyl alcohol

SEM - Scanning electron microscopy

TMZ - Temozolomide

Tf - Transferrin

TGF-β1 - Transforming growth factor-β1

TP53 - Tumour protein p53

W/o/w - Water-in-oil-in-water

WHO - World Health Organization

Acknowledgments

I would like to thank Dr. Mohsen Akbari for his support, and encouragement throughout my study and research. Without his insightful guidance, the work leading to the creation of this thesis could not have been successfully conducted.

I would like to express my sincere appreciation to Dr. Stephanie Willerth for kindly giving me the opportunity to use her lab facilities.

My gratitude goes to my fellow lab members for their encouragement, support, and friendship. In particular, Bahram, Erik, and Nahiane for assisting me in the experimental part of this work, Bahram, Brent, and Lucas for their constructive feedback on my thesis.

Last but not the least, I would like to express my sincere gratitude to my family: my parents and brothers for supporting me spiritually throughout my life.

Dedication

I dedicated this to my mother for her ongoing love and endless support.

Introduction

A collection of abnormal cells within the brain is known as a brain tumour. Generally, brain tumours are divided into two categories based on their origin; primary and secondary. Primary brain tumours stem from cells within the brain whereas secondary brain tumours are those that begin elsewhere in the body and then spread into the brain (Lesniak & Brem, 2004; Woodworth, Dunn, Nance, Hanes, & Brem, 2014). Gliomas stem from neuroglial progenitor cells and have been organized into a four-tiered histological grading scheme by the World Health Organization (WHO) (Woodworth et al., 2014). Glioblastoma multiforme (GBM) is a grade IV glioma (most malignant form) and accounts for 60-70% of all glial tumours (Jawhari, Ratinaud, & Verdier, 2016). More than half of the 21,800 patients diagnosed with primary brain tumours in the United States suffer from GBM which has a mean survival rate of less than one year from the time of diagnosis (Dilnawaz & Sahoo, 2013; Pourgholi, hajivalili, Farhad, Kafil, & Yousefi, 2016). Studies reported that GBM incidence rate increases in aging populations and it peaks among 70 to 84 years age group (Figure 1) (Thakkar et al., 2014). On the other hand, this aggressive type of brain tumour accounts for only 3% of all brain and central nervous system tumours among 0 to 19 age group. A shorter survival rate has been reported for patients who are older than 70. The main reasons for the shorter survival rate post-diagnosis are the poor ability in tolerating neurological insults associated with surgery and/or adjuvant therapy, and comorbid conditions in the elderly (Thakkar et al., 2014).

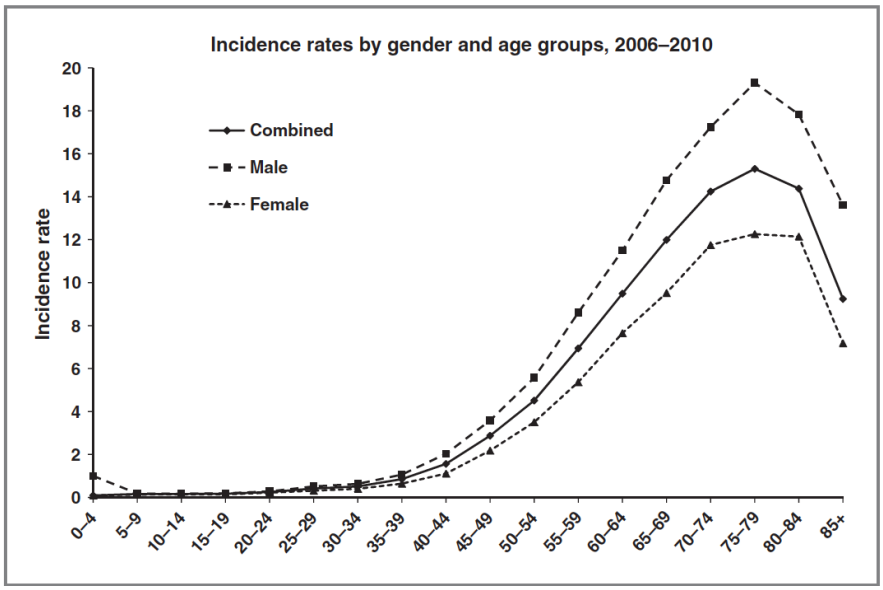

Figure 1. The effect of gender and age on the incidence rate of GBM (incidence rates are per 100,000). Reproduced with permission (Thakkar et al., 2014).

Primary GBM arises de novo, without any gradual progression from low-grade astrocytoma (II or III) as opposed to secondary GBM which is developed from low-grade astrocytoma (Figure 2) (Jawhari et al., 2016; Lesniak & Brem, 2004).

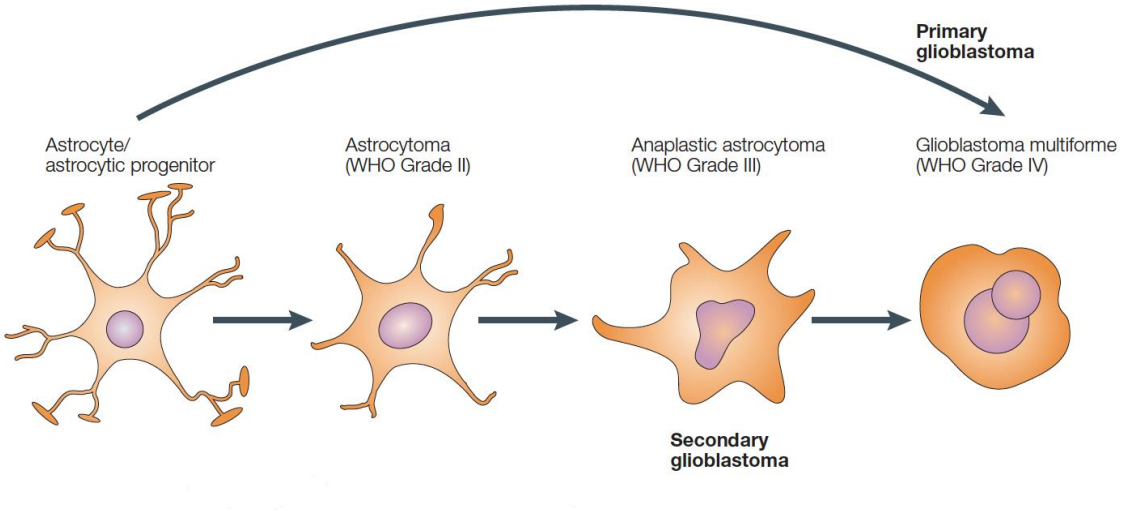

Figure 2. Development of GBM with or without gradual progression from low-grade astrocytoma. Reproduced with permission (Lesniak & Brem, 2004).

Primary GBM constitutes over 90% of these tumours and is more prevalent in patients over the age of 60 (Jawhari et al., 2016). Although studies demonstrated that primary and secondary GBM have similar morphology, they develop through different genetic pathways (Ohgaki & Kleihues, 2007). Primary GBM is genetically characterized by the overexpression of epidermal growth factor receptor (EGFR) (36%), deletion of p16 cyclin-dependent kinase inhibitor 4a (p16INK4a) (31%), and mutations of phosphatase and tensin homolog (PTEN) (25%) (Jawhari et al., 2016; Ohgaki & Kleihues, 2007). In contrast, tumour protein p53 (TP53) gene mutations (65%) are the most common genetic alterations in those who suffer from secondary GBM (Figure 3) (Jawhari et al., 2016; Ohgaki & Kleihues, 2007).

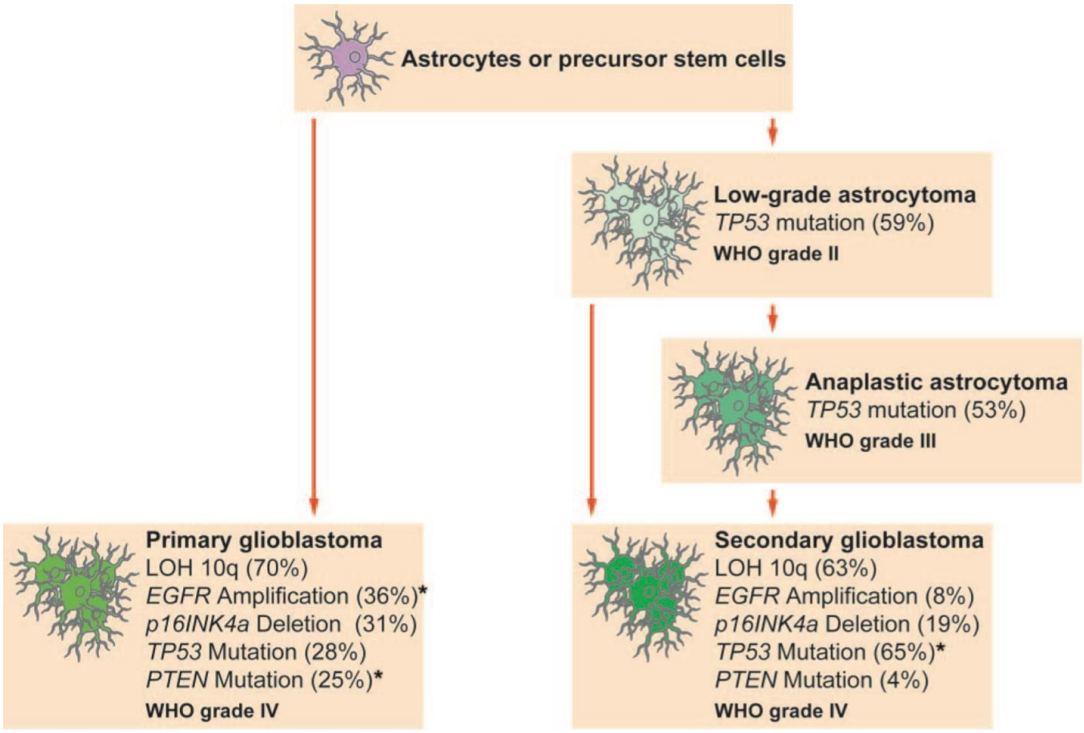

Figure 3. Genetic pathways involved in the development of primary and secondary GBM. Reproduced with permission (Ohgaki & Kleihues, 2007).

Despite advances in surgical neuro-oncology, the treatment of GBM remains a significant challenge (Combs et al., 2008). The diffuse nature of high-grade gliomas makes

the complete removal of the tumour by surgery without damaging the surrounded healthy tissue almost impossible (Stewart, 2002). It has been reported that surgical resection alone contributes to a median survival of 6 months (Wilson, Karajannis, & Harter, 2014). Radiotherapy post-surgery could only extend the median survival to 12.1 months because of the resistance of hypoxic regions within this aggressive tumour to the radiation (Flynn et al., 2008; Wilson et al., 2014). After surgical resection, chemotherapy combined with radiotherapy, which is the standard treatment for GBM, prolongs the median survival to 14.6 months (Stupp et al., 2005). However, there are numerous deficiencies associated with the administration of chemotherapeutic agents. The blood-brain barrier (BBB), composed of endothelial cells joined by tight junctions, separates the central nervous system from other parts of the body (Figure 4). Due to the presence of this barrier, the number of chemotherapy drugs effective in the treatment of GBM is limited (Wohlfart, Gelperina, & Kreuter, 2012).

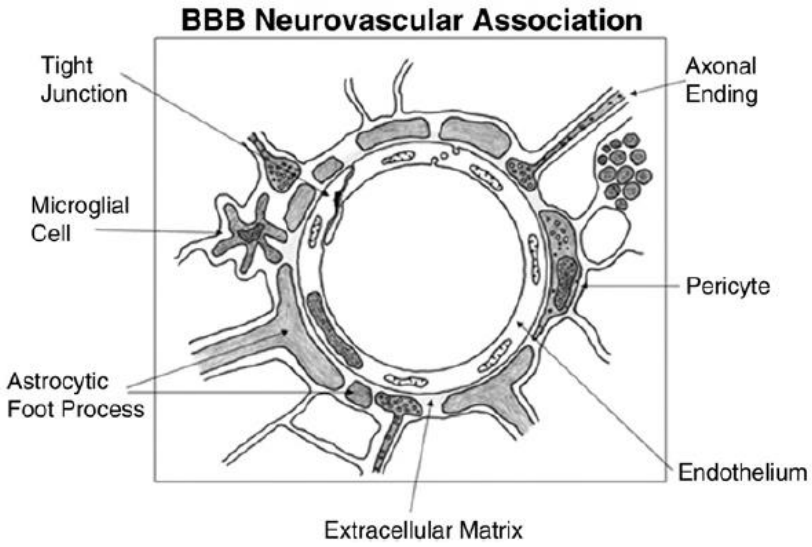

Figure 4. Structure of the blood-brain barrier. Reproduced with permission (Wohlfart et al., 2012).

Temozolomide (TMZ) is the most commonly used chemotherapeutic agent in the treatment of GBM due to its capability to pass the BBB relatively easily (Ananta et al., 2016).

However, its short half-life in plasma, about 1.8 hours, necessitates high systemic administration doses. Prolonged oral administration of TMZ along with high oral doses lead to numerous side effects in GBM patients such as nausea, vomiting, fatigue, headache, and lymphopenia (Ananta et al., 2016; H. Zhang & Gao, 2007). The aforementioned shortcomings associated with traditional methods contribute to the recurrence of GBM within 2 cm of the original tumour in 80% of patients (Guerin, Olivi, Weingart, Lawson, & Brem, 2004). Thus, developing novel treatment strategies is an unmet demand. A drug delivery system incorporated with a chemotherapeutic agent that delivers the drug directly to the tumour site is an effective method which can extend the half-life by keeping the drug intact within itself, enhance the treatment efficacy, and also reduce the systemic toxicity (Duntsch, 2009; Fourniols et al., 2015).

This thesis has focused on developing a drug-eluting 3D bioprinted mesh (GlioMesh) capable of releasing TMZ over one month at the tumour site and thus reducing the chance of GBM recurrence. After an overview of the conventional and new strategies for the treatment of GBM, polymeric microsphere fabrication and 3D bioprinting by which GlioMesh has been developed will be described. Finally, the GlioMesh will be introduced, and its main characteristics will be discussed.

Chapter 1: Treatment Strategies for GBM

One of the significant causes of global mortality is cancer. It has been predicted that 15 million patients will be diagnosed with cancer by 2020 among which 12 million would die because of the consequences of this devastating disease (Pourgholi et al., 2016). GBM accounts for about 77% of all malignant brain tumours and is among the most aggressive cancers in human beings (Pourgholi et al., 2016). Although the most intense treatment regimens used for GBM patients, they rarely live over two years (Pourgholi et al., 2016; Woodworth et al., 2014). In the first section of this chapter, a brief review of the conventional strategies for the treatment of GBM patients including surgery, radiotherapy, and chemotherapy will be provided. Surgical resection alone contributes to a median survival of only 6 months because of the infiltrative nature of GBM (Lesniak & Brem, 2004). The median survival of GBM patients is prolonged to 12.1 months when surgery is combined with radiotherapy. The inherent and acquired insensitivities to radiation diminish the effectiveness of this method of treatment (Gökhan Eğilmez, Gürsel A. Süer,Özgüner, 2012). Post-surgical radiotherapy along with chemotherapy further extend the median survival to 14.6 months (Wilson et al., 2014). Despite the treatment methods discussed, the five-year overall survival of GBM patients is only 9.8%. As described previously, the BBB inhibits the entrance of most of the orally administered chemotherapy drugs into the tumour site and thus reduces the treatment efficacy (Gökhan Eğilmez, Gürsel A. Süer,Özgüner, 2012).

Since gliomas rarely metastasize outside the central nervous system and usually return within 1-2 cm of the original site after resection, delivering chemotherapeutic agents directly to the tumour site is a promising approach to eradicate the residual tumour cells

(Gökhan Eğilmez, Gürsel A. Süer,Özgüner, 2012; Woodworth et al., 2014). Subsequent sections of this chapter will be focused on the pros and cons of localized and targeted drug delivery systems to deliver the potent chemotherapeutic agent to the tumour site. In general, these methods of treatment could increase the treatment efficacy by providing a higher concentration of drug at the desired area while minimizing the systemic toxicity.

1.1. Conventional strategies for the treatment of GBM

1.1.1. Surgery

Surgery is crucial in the initial treatment of GBM (Hou, Veeravagu, Hsu, & Tse, 2006). This technique of treatment has several benefits including reducing mass effect from tumour tissue, cytoreduction, and also providing tissue specimens for histological analysis (Black, 1998; Hou et al., 2006; Omuro & DeAngelis, 2013). Magnetic resonance imaging (MRI) and computed tomography (CT) scans are usually used for visualization of a brain tumour before conducting surgery (Chamberlain & Kormanik, 1998). It has been reported that the extent of surgical resection, ranging from biopsy to subtotal to total, affects the overall survival of patients. Total resection usually doubles the length of survival to approximately 11-12 months compared to biopsy alone (Adamson et al., 2009; Hou et al., 2006). However, invasive surgery with the aim of removing the total tumour mass is not usually suggested since it may be associated with serious neurological insults to the surrounding normal tissue (Stewart, 2002). It has been reported that the complete removal of this aggressive tumour is almost impossible due to the diffuse nature of GBM. Florescent-guided surgery in which agents such as d-aminolevulinic acid have been used to label tumour cells showed modest advances in removing the migrated cells (Adamson et al., 2009).

1.1.2. Radiotherapy

The first post-surgery adjuvant therapy method for GBM was radiotherapy in the form of whole brain radiation. Studies reported that radiation therapy typically doubles the survival rate from 4-6 months to 10-11 months. However, the sensitivity of some of the critical central nervous system structures including frontal lobes, optic apparatus, and brain stem to radiation limits the maximum whole brain radiation therapy dose. Localizing radiation therapy to the desired area of the body is the main adjustment that has been applied to this method of treatment for GBM. Studies demonstrated that fractionated focal radiation technique which provides a high dose to the targeted area is as effective as whole brain radiation therapy while reducing the negative consequences associated with this method of treatment. Recently, the intensity modulated radiation therapy, which allows dose escalation to the targeted tumour site without compromising normal tissue, has been widely used for patients with GBM (Chao et al., 2001). Radiation therapy with this approach is typically divided into a daily dose of 2 Gy given 5 days per week for up to 1.5 months (Adamson et al., 2009; Woodworth et al., 2014). Despite the survival benefits achieved by radiotherapy in the treatment of GBM, hypoxia, which is one of the characteristic features of GBM, results in resistance to radiation therapy. In general, oxygen improves the effectiveness of a given dose of radiation through the formation of DNA-damaging free radicals (Flynn et al., 2008).

1.1.3. Chemotherapy

Chemotherapy can be administered either alone or as a supplement to other approaches for GBM treatment (Hou et al., 2006). The most widely used method of treatment for children under the age of 3 is neo-adjuvant chemotherapy. In this technique,

the chemotherapeutic agent is administered immediately after surgical resection and before radiotherapy. Chemotherapy drugs may also be used at the same time with radiotherapy with the aim of sensitizing the brain tumour to the impacts of radiation therapy, this method of treatment is known as chemoradiosensitization. Furthermore, several studies reported considerable improvements in the treatment of malignant gliomas when the chemotherapeutic agent is prescribed after surgery and radiotherapy as adjuvant therapy (Chamberlain & Kormanik, 1998). Nitrosoureas, such as 1,3-bis(2-chloroethyl)-1-nitrosourea (BCNU), have been dominated the adjuvant chemotherapy method over several years since they can cross the intact BBB due to their lipophilicity (Stewart, 2002). The University of California, San Francisco, Neuro-Oncology Service reported that surgery followed by radiation therapy contributed to 44% one-year survival, 6% three-year survival, and 0% five-year survival in patients who were suffering from GBM. On the other hand, postoperative radiotherapy followed by adjuvant chemotherapy with nitrosourea demonstrated a one-year survival of 46%, three-year survival of 18%, and five-year survival of 18% (Chamberlain & Kormanik, 1998).

TMZ, which is an orally-administered DNA-alkylating agent, has been reported as the main chemotherapy drug for GBM (Pourgholi et al., 2016; J. Zhang, Stevens, & Bradshaw, 2012). This chemotherapeutic agent has the same efficacy as BCNU while exhibiting less toxicity (Adamson et al., 2009). TMZ works as a prodrug in which the more alkaline brain tumour pH compared to nearby healthy tissue contributes to this alkylating agent activation (J. Zhang et al., 2012). Figure 5 demonstrates the mechanism of activation of TMZ within the tumour tissue. The hydrolytic ring opening of tetrazinone results in the formation of an active compound: monomethyl triazene 5-(3-methyltriazen-1-yl)-

imidazole-4-carboxamide (MTIC). Subsequently, as the result of MTIC reaction with water the considerably reactive methyldiazonium ion would be formed. Finally, the methyldiazonium ion prevents DNA replication through methylation of purine groups of DNA such as O6-guanine, N7-guanine, and N3-adenine (Newlands, Stevens, Wedge, Wheelhouse, & Brock, 1997; Wheelhouse & Stevens, 1993; J. Zhang et al., 2012).

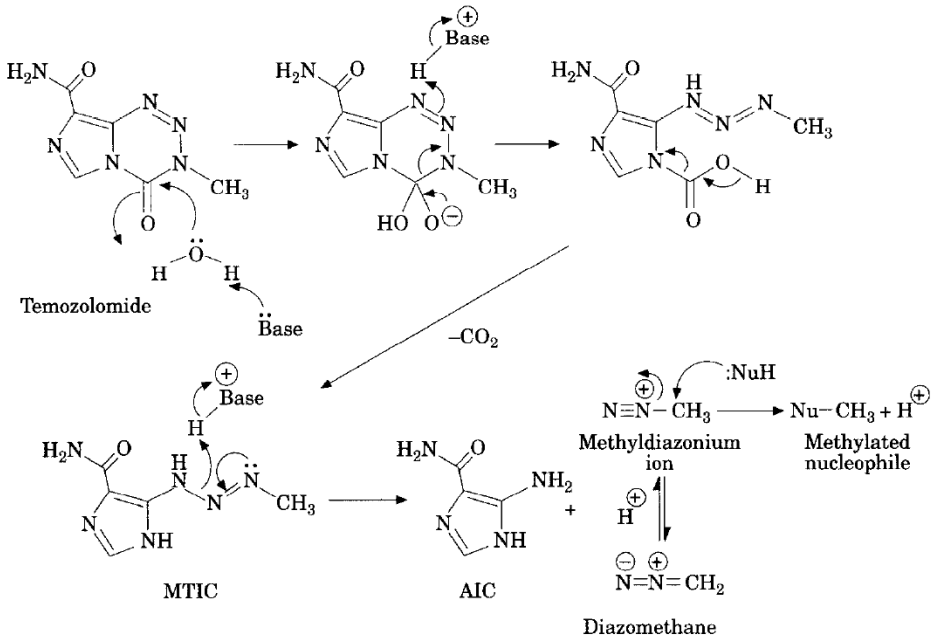

Figure 5. TMZ activation mechanism. Reproduced with permission (Newlands et al., 1997).

Stupp *et al.* demonstrated that radiation therapy plus concomitant and adjuvant TMZ therapy could provide a considerable survival benefit for patients with newly diagnosed glioblastoma. 573 patients from 85 institutes were randomized to receive either radiotherapy alone or radiotherapy plus continuous daily TMZ administration, followed by adjuvant TMZ therapy. Patients treated with radiation therapy alone showed a median survival of 12.1 months, whereas those who received radiotherapy plus TMZ demonstrated the median survival of 14.6 months. Moreover, the two-year survival was 10.4% in the

group treated with radiotherapy alone, as compared with 26.5% in the group treated with radiation therapy plus TMZ (Figure 6) (Stupp et al., 2005).

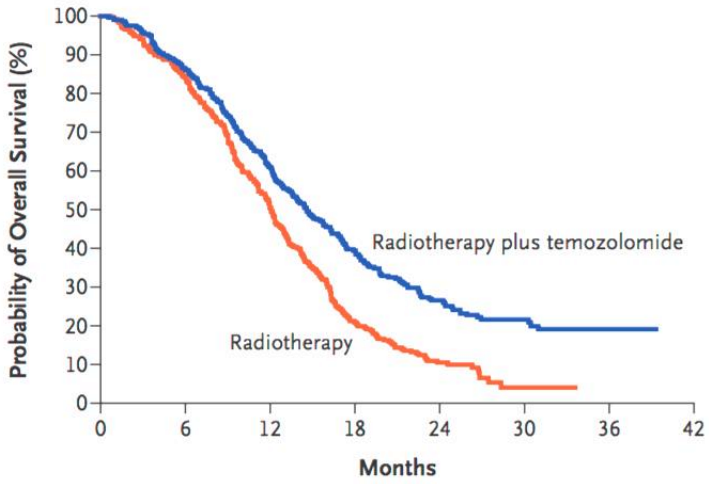

Figure 6. The effect of radiotherapy versus radiotherapy plus TMZ on the probability of overall survival. Reproduced with permission (Stupp et al., 2005).

In spite of the achieved survival benefits by chemotherapeutic agents that are capable of passing the BBB, the shortcomings associated with systemic administration of these chemotherapy drugs limit their potential usage (Hou et al., 2006; Pourgholi et al., 2016). They are usually needed to be administered in high oral doses to reach the therapeutic levels of the brain because of their short half-life. This, along with their prolonged systemic administration, contributes to several side effects including nausea, vomiting, fatigue, headache, pulmonary fibrosis, and myelosuppression (Ananta et al., 2016; Woodworth et al., 2014; H. Zhang & Gao, 2007).

1.2. Novel strategies for the treatment of GBM

1.2.1. Gliadel® wafer

As described previously, GBM has a median survival of almost one year despite the maximum treatment with surgery, radiotherapy, and chemotherapy. Recurrence of GBM within 2 cm of the original tumour in 80% of cases necessitates the development of

a drug delivery system that can provide high chemotherapy drug concentration at the tumour site (Guerin et al., 2004). Gliadel® wafer is an interstitial local chemotherapy which was approved by the US Food and Drug Administration as a supplement to surgical resection for recurrent glioblastoma and also as the initial treatment for glioblastoma in 1996, and 2003, respectively (Guerin et al., 2004). This biodegradable polymer-based drug delivery system is composed of 3.85% BCNU in poly-[bis-p-(carboxyphenoxy)propane-sebacic acid] copolymer (PCPP-SA) (Guerin et al., 2004; Westphal, Ram, Riddle, Hilt, & Bortey, 2006). In this treatment procedure, eight dime-size Gliadel® wafers are placed into the resection cavity at the time of surgery and then secured in place by using Surgicel®, which is a blood-clot-inducing material (Figure 7).

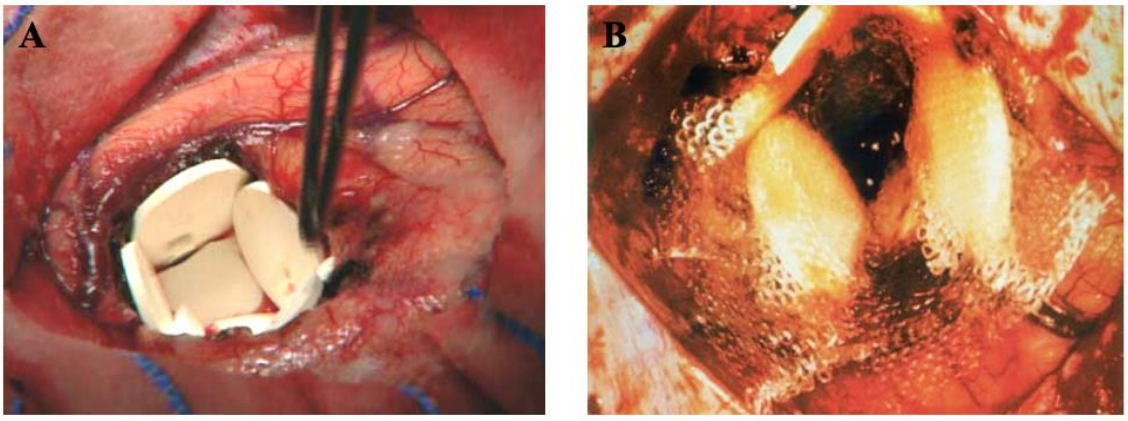

Figure 7. Implantation of Gliadel® wafer. (A) Placement of eight dime-size poly-anhydride wafers at the resection cavity after surgical operation. (B) Securement of poly-anhydride biodegradable wafers in their place with Surgicel®. Reproduced with permission (Guerin et al., 2004; Lesniak & Brem, 2004).

These wafers are capable of releasing BCNU in a sustained manner over a 2-3 weeks period, improving the GBM patients treatment efficacy, and also alleviating the side effects associated with oral administration of BCNU including pulmonary fibrosis and myelosuppression (Woodworth et al., 2014). Although these wafers provide several advantages in GBM treatment, there are numerous limitations associated with the

administration of this localized drug delivery carrier which should be taken into account. The size and rigidity of wafers prevent their conformal contact with the brain tissue and utilization of the entire resection cavity. This, in turn, results in a non-homogenous BCNU distribution and leaving some of the cancer cells untreated (Kennedy & Curtis, 2002). Additionally, it has been reported that Gliadel® wafers are beneficial in the treatment of GBM only if a tumour is unifocal and unilateral (Guerin et al., 2004). Lastly, cerebral oedema occurrence after the implantation of these wafers by surgery necessitates a high dose steroid therapy with dexamethasone up to two weeks which would affect the patients' quality of life (Guerin et al., 2004).

1.2.2. Polymeric microspheres

In spite of the benefits offered by Gliadel® wafers in the treatment of GBM including bypassing the BBB, providing higher local BCNU concentration, and minimizing the systemic toxicity, the size of Gliadel® wafers limits the administration to invasive surgical operation. Development of polymer-based microspheres loaded with chemotherapy drugs could provide the same benefits as Gliadel® wafers in the treatment of GBM patients. However, the smaller size of microspheres eliminates the need for conducting invasive surgeries (Figure 8) (Gil-Alegre, González-Álvarez, Gutiérrez-Paúls, & Torres-Suárez, 2008).

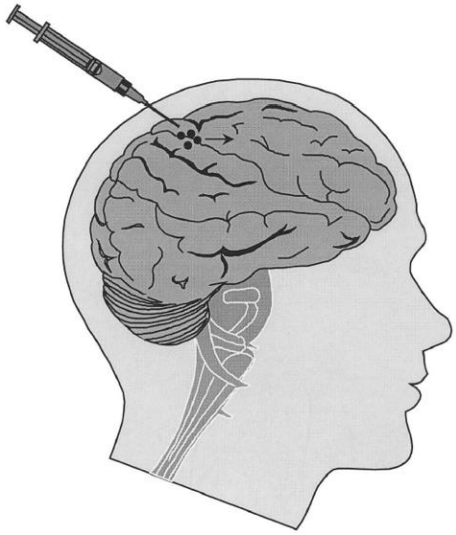

Figure 8. Polymeric microspheres administration with a needle through cerebral stereotactic surgery. Reproduced with permission (Gutman, Peacock, & Lu, 2000).

Poly (d, l-lactide-co-glycolide) (PLGA) is a well-known biocompatible and biodegradable polymer approved by the US Food and Drug Administration for medical applications (Ananta et al., 2016). The biodegradation of microspheres fabricated from PLGA circumvents the need for surgical removal of the implanted carriers after treatment (Daniel, Brouillard, & Benoit, 1993). Furthermore, the relative hydrophobicity of PLGA inhibits the interaction of the incorporated agent with the surrounding aqueous environment and thus keeps the drug protected within the carrier (Wu & Ding, 2004). Encapsulated therapeutic agents within the aforementioned microspheres generally release through diffusion, erosion mechanism, or a combination of both. Erosion mechanism happens via hydrolysis of ester linkages within the PLGA backbone (Zolnik & Burgess, 2007). Gil-Alegre *et al.* fabricated BCNU-loaded PLGA microspheres for intracranial administration by using an oil-in-water (o/w) emulsion solvent evaporation method. Their studies demonstrated that PLGA microspheres are capable of releasing BCNU over 21 days mainly through diffusion (Figure 9).

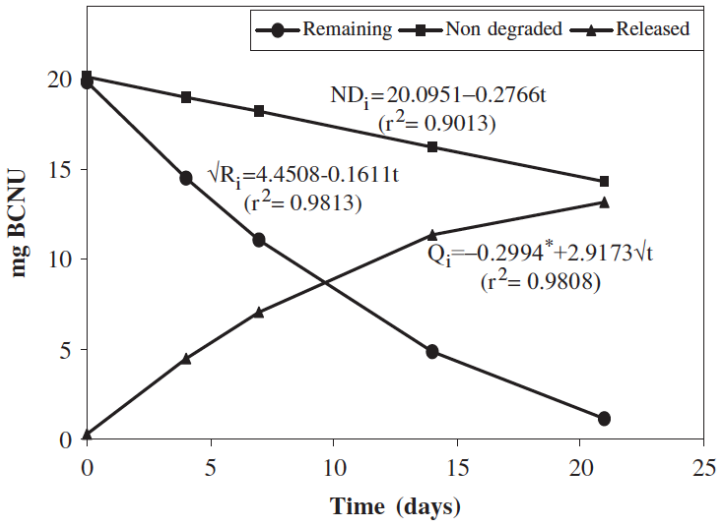

Figure 9. *In vitro* BCNU release from PLGA microspheres. Reproduced with permission (Gil-Alegre et al., 2008).

By conducting *in vitro* cell viability tests, they observed that the released BCNU from PLGA microspheres 21 days after their administration contributed to approximately 60% reduction in the viability of human glioblastoma cell line (U-373 MG) (Figure 10) (Gil-Alegre et al., 2008).

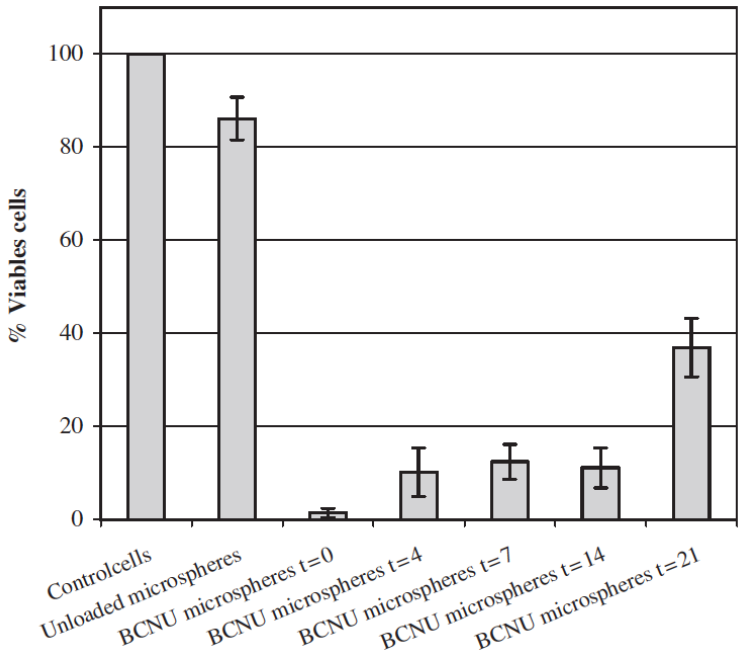

Figure 10. The cytotoxic effect of BCNU-loaded PLGA microspheres to U-373 MG cells *in vitro*. Reproduced with permission (Gil-Alegre et al., 2008).

The same efficacy of TMZ to BCNU in the GBM treatment, while its reduced toxicity encouraged the researchers to encapsulate TMZ within PLGA microspheres (Adamson et al., 2009). Previous studies reported low encapsulation efficiencies for the prepared TMZ-loaded PLGA microspheres by o/w and water-in-oil-in-water (w/o/w) emulsion solvent evaporation method (Table 1). The rapid diffusion of amphiphilic TMZ from the internal phase to the external water phase during the fabrication process accounted for the obtained low encapsulation efficiencies (Ananta et al., 2016).

Table 1. The effect of different emulsion methods and TMZ concentrations on the encapsulation efficiency of TMZ-loaded PLGA microspheres. Reproduced with permission (Ananta et al., 2016).

Method	TMZ concentration (%, w/v)	Encapsulation efficiency (%)
o/w	20	2
o/w	40	1.5
o/w	80	1.25
w/o/w	10	6
w/o/w	20	4.5
w/o/w	40	3.5

Therefore, future studies should be focused on improving the encapsulation of TMZ within PLGA microspheres to reduce the amount of required drug for microsphere fabrication and make the process more cost-effective. The other deficiency associated with the use of polymeric microspheres in the treatment of GBM is their high surface energy which leads to aggregation and makes the injection through stereotactic surgery difficult. Lastly, the injected microspheres tend to migrate away from the tumour site because of cerebral flow which results in reducing the effectiveness of this localized drug delivery method (Daniel et al., 1993).

1.2.3. Convection-enhanced delivery

Generally, the proliferation of cells which have migrated from the tumour focus leads to GBM recurrence. It has been reported that localized therapy such as administration of Gliadel® wafers and drug-loaded polymeric microspheres have considerable difficulties in targeting distant invading cancer cells (Adamson et al., 2009). Limited drug penetration from the diffusive interface of these diffusion-mediated drug delivery devices makes them less effective in targeting the migrated cells (Adamson et al., 2009; Giaouris, E., Chorianopoulos, N., Skandamis, P. y Nychas, 2012). Catheter-based convection-enhanced delivery (CED) is a promising localized drug delivery method which provides the advantage of crossing the BBB, distributing chemotherapy drugs to areas as large as the entire cerebral hemisphere and thus attacking the distant invading cells (Woodworth et al., 2014). In this method of treatment, the required pressure gradient is provided by a motor-mediated pump which is connected to the catheter. The pressure gradient at the tip of the fine catheter which is implanted at the time of stereotactic surgery allows for delivering the agent directly into the interstitial space of central nervous system (Figure 11) (Giaouris, E., Chorianopoulos, N., Skandamis, P. y Nychas, 2012).

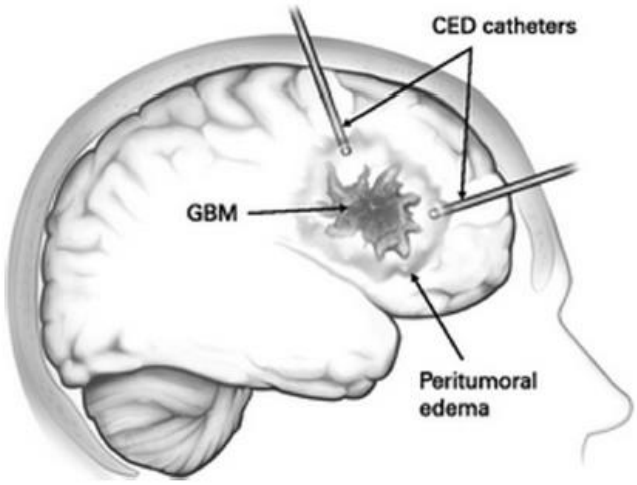

Figure 11. Insertion of CED through bur holes into the interstitial spaces of the brain. Reproduced with permission (Mehta, Sonabend, & Bruce, 2017).

It has been reported that pressure-mediated CED contributes to the homogenous distribution of therapeutic agents over a large area of the brain through displacing interstitial fluid with the infusates (Adamson et al., 2009; Giaouris, E., Chorianopoulos, N., Skandamis, P. y Nychas, 2012; Woodworth et al., 2014). Additionally, CED can deliver a wide range of agents with various molecular weights including conventional chemotherapeutics, small molecule inhibitors, and immunotoxins (Giaouris, E., Chorianopoulos, N., Skandamis, P. y Nychas, 2012; Mehta et al., 2017). Zvi *et al.* evaluated the effectiveness of intramural CED of paclitaxel, an antitumour agent, in 15 patients with histologically confirmed recurrent GBM. They administered a total of 20 cycles of CED of paclitaxel into the patients and used diffusion-weighted (DW) MRI on a daily basis to assess the convective process. Their results demonstrated that 5 out of 15 patients responded significantly and 6 of the patients had a partial response of 73%. They believed that the reason for observing a poor response in a few of cases was paclitaxel backflow into unwanted areas such as subarachnoid spaces, ventricles, and previously formed resection cavities (Zvi et al., 2004).

Treatment of brain tumour via catheter-based CED method is not without deficiencies. As mentioned previously, one of the main challenges for the usage of CED in clinical applications is backflow along the catheter (Giaouris, E., Chorianopoulos, N., Skandamis, P. y Nychas, 2012; Woodworth et al., 2014). Studies demonstrated that the incidence of delivered agent reflux is dependent on several factors including the size, shape, and the technique of implantation of the catheter. Reduction in the drug concentration at the desired site along with chemical meningitis due to drug leakage in unintended areas, such as the subarachnoid space, are the shortcomings attributed to backflow along the catheter (Giaouris, E., Chorianopoulos, N., Skandamis, P. y Nychas, 2012).

1.2.4. Nanoparticles

As previously stated, the presence of the BBB provides a formidable challenge for chemotherapeutic agent delivery to brain tumours. However, studies reported that restrictions applied by the BBB in delivering chemotherapy drugs are not insurmountable (Lucienne Juillerat-Jeanneret, 2008; Lockman, Mumper, Khan, & Allen, 2002). Administration of localized drug delivery systems such as Gliadel® wafers, polymeric microspheres, and CED helps to ferry drugs across the BBB, but improvements in these methods are required. Alteration of the integrity of the BBB has been suggested as another possible approach to circumvent this barrier and can be accomplished by the opening of its tight junctions through the employment of either artificial osmotic pressure or bradykinin analogues such as RMP-7. However, the mentioned approach results in the entrance of toxins and unwanted molecules to the central nervous system (Lockman et al., 2002).

Colloidal carriers, specifically, biodegradable polymeric nanoparticles are considered as a promising option for transporting therapeutic agents across the intact BBB

(Lockman et al., 2002; Wohlfart et al., 2012). Targeted drug delivery provided by the administration of nanoparticles, as opposed to localized drug delivery approaches reduces the chance of healthy tissue exposure to chemotherapy drugs. This method of treatment can be divided into two different categories, active and passive. Passive targeting is based on anatomical variances between healthy and diseased tissues (L. Juillerat-Jeanneret & Schmitt, 2007; Pourgholi & Farhad, 2016). Following administration, nanoparticles smaller than 80 nm could pass the BBB due to increased permeability of the BBB impaired by brain tumour growth. Increased movements of nanoparticles through wider fenestrations in the immature vasculature accounts for their accumulation within the tumour tissue (Lucienne Juillerat-Jeanneret, 2008; Woodworth et al., 2014). On the other hand, active targeting usually occurs through receptor-mediated pathways (Lockman et al., 2002; Michaelis, 2006; Wohlfart et al., 2012). In this procedure, surface modification of nanoparticles by covalently bound targeting ligands, or coating with specific surfactants, allows for adsorption of specific plasma proteins required for receptor-mediated uptake (Wohlfart et al., 2012). For example, it has been reported that GBM cells have a relatively high number of low-density lipoprotein receptors (LDLR) as opposed to normal neurons. Thus, one can simply use the upregulation of LDLR to deliver agents to the tumour cells (Pourgholi et al., 2016). Kreuter *et al.* reported that polysorbate 80 coated nanoparticles administered intravenously could adsorb the plasma apolipoprotein E (Apo E) on their surface. Apo E is a protein which facilities the transport of lipids into the brain via LDLR. Therefore, these nanoparticles can mimic the lipid molecules which interact with LDLR on the brain capillary endothelial cells (Kreuter et al., 2002). The effectiveness of polysorbate 80 coated nanoparticles on 101/8 glioblastoma in rats, a morphologically

similar tumour to human glioblastoma, was evaluated by Steiniger *et al.* They observed that intravenous administration of doxorubicin-loaded poly (butyl cyanoacrylate) (PBCA) nanoparticles coated with polysorbate 80 contributes to a long-term survival (>180 days) in approximately 20-40% of treated rats (Steiniger et al., 2004). In spite of the mentioned advantages of using nanoparticles in brain tumour treatment, there are several major concerns regarding the administration of brain tumour targeting drug delivery systems. The U87 brain tumour has a pore size of about 7-100 nm. This results in difficulties for the transportation of nanoparticles with a size higher than 100 nm across the BBB. Additionally, a protein corona forms followed by the introduction of nanoparticles to biological fluids. This protein corona is able to cover the ligands and thus inhibits the reaction between the ligands and their receptors (Gao, 2016). Salvati *et al.* incubated nanoparticles modified with transferrin (Tf) by a serum-containing cell culture media and observed a considerable reduction in the reaction between Tf and its corresponding receptor on cells due to the formation of protein corona (Salvati et al., 2013). The other limitation of nanoparticle therapy is off-target effects. Although TF receptor is upregulated on brain tumour cells, it is also expressed on other cells at different levels which results in inevitable off-target effects (Gao, 2016).

1.3. Conclusion

GBM is the most prevalent and devastating primary brain tumour in adults. Although the standard of care for treatment of GBM is surgical resection followed by radiotherapy accompanied by chemotherapy, the prognosis of GBM patients remains very poor. The inherent resistant and sheltering environment of brain tumour are the main challenges that reduce the effectiveness of conventional methods of treatment. GBM has a

diffuse nature which hinders the removal of tumour mass entirely during surgical intervention. Additionally, hypoxic regions make the tumour cells insensitive to radiation therapy. Moreover, the presence of the BBB limits the number of effective chemotherapy drugs for the treatment of GBM. TMZ is the most widely used chemotherapeutic agent in GBM treatment because of its ability to cross the BBB. However, the short half-life of this chemotherapy drug in plasma requires high systemic administration doses to reach the brain with therapeutic efficacy. Several side effects have been observed in GBM patients due to high doses and prolonged systemic administration of TMZ which restrict its potential use in GBM treatment.

The aforementioned inadequacies associated with traditional methods of treatment makes the recurrence of GBM inevitable. This makes the development of novel strategies which can ferry the chemotherapy drug across the BBB and therefore, enhance therapeutic efficacy an urgent need. Localized and targeted drug delivery systems hold great promise in GBM treatment because of their capability to provide a high concentration of chemotherapeutic agent at the desired site and thus decreasing the systemic toxicity. Each of these avenues for GBM treatment has their own benefits and drawbacks. Gliadel® wafer is a commercially available localized drug delivery system for GBM which provides the advantage of circumventing the BBB. However, the size and rigid nature of these wafers result in numerous complications for implantation and utilization of the entire resection pocket. As opposed to Gliadel® wafers which require invasive surgeries for placement, the smaller size of drug-loaded polymeric microspheres makes their multiple administration with minimally invasive stereotactic surgery possible. However, this method of treatment is not without limitations. Low encapsulation of chemotherapeutic agents such as TMZ

within PLGA microspheres suggests that the current format of these carriers does not provide much advantage in GBM treatment. Diffusion-mediated drug delivery vehicles such as Gliadel® wafer, and polymeric microspheres, do not have the capability of attacking distant invading tumour cells due to the limited penetration of agent from the diffusive interface. Although the homogenous distribution of drug over a vast region of brain achieved by pressure-driven CED allows for delivering the chemotherapy drug into the migrated cells, the backflow along CED has posed significant restrictions for its use in the clinical arena. Targeted drug delivery systems have been developed to reduce the chance of surrounding healthy tissue exposure to chemotherapeutic agents. Surface modification of drug-loaded nanoparticles enables their entry to the tumour cells after administration through receptor-mediated pathways. However, studies reported that the presence of same receptors on the healthy cells contributes to off-target effects in some cases. Therefore, the current design of nanoparticles cannot guarantee to deliver the chemotherapeutic agents to tumour cells only.

Chapter 2: Fabrication of Polymeric Microspheres

In the 1960s, polymers such as silicon rubber and polyethylene were suggested as delivery carriers to obtain a controlled release of therapeutic agents (Freiberg & Zhu, 2004). However, these systems required to be removed eventually by conducting surgeries because of not being degradable (Freiberg & Zhu, 2004). The idea of using biodegradable polymers as drug delivery vehicles to circumvent the removal step by operation dates back to the 1970s (Freiberg & Zhu, 2004). Microspheres, micro-scale particles often made of biodegradable polymers, have been widely used as drug delivery devices. Polyesters such as poly (lactic acid) (PLA) (Bodmeier & McGinity, 1988; Wakiyama, JUNI, & NAKANO, 1982), and PLGA (Gil-Alegre et al., 2008; H. Zhang & Gao, 2007) are commonly used for the fabrication of drug-loaded microspheres due to their biodegradability, biocompatibility, low immunogenicity, and reduced toxicity. Approval of PLGA for use in human by the US Food and Drug Administration made this polymer more attractive in the fabrication of microspheres (Table 2) (Iqbal, Zafar, Fessi, & Elaissari, 2015). In addition, favourable mechanical properties and predictable biodegradation of PLGA have resulted in its widened role in biomedical applications (Uchegbu & Schatzlein, 2006).

Table 2. Microspheres formulations approved for use in humans. Reproduced with permission (Uchegbu & Schatzlein, 2006).

Active ingredient	Product name	Polymer	Drug release (months)
Leuprorelin acetate	Lupron Depot®	PLGA	3
Leuprorelin acetate	Prostap® 3	PLGA	3
Octreotide acetate	Sandostatin LAR®	PLGA-glucose	1

Triptorelin pamoate	Trelstar™ Depot	PLGA-polyethylene glycol	1
Triptorelin pamoate	Decapeptyl®	PLGA	1
Lanreotide acetate	Somatuline® LA	PLGA	0.5

Drug release from PLGA microspheres occurs via diffusion, erosion of the polymer, or a combination of the two. This depends on polymer properties such as molecular weight, copolymer composition, crystallinity, and some of the drug delivery system characteristics, including size, porosity, and drug loading (Zolnik, Leary, & Burgess, 2006). PLGA microsphere erosion happens via hydrolysis of the ester linkages following exposure to an aqueous environment (Figure 12) (Zolnik & Burgess, 2007). This erosion results in the production of biocompatible lactic and glycolic acids (Iqbal et al., 2015).

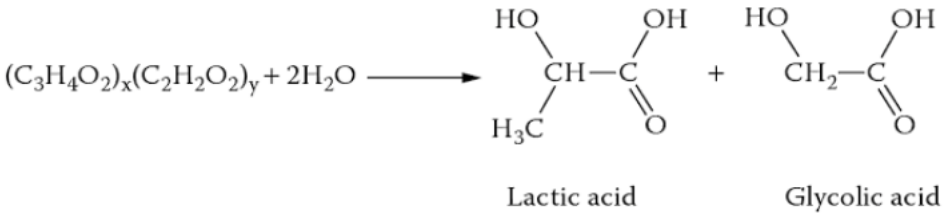

Figure 12. Hydrolysis mechanism of PLGA. Reproduced with permission (Uchegbu & Schatzlein, 2006).

Several emulsion solvent evaporation techniques have been developed for encapsulation of therapeutic agents within polymeric microspheres and selection of one method over the other considerably depends on the solubility of the agent (Uchegbu & Schatzlein, 2006). Single o/w emulsion solvent evaporation technique has been commonly used to encapsulate hydrophobic drugs such as chlorpromazine (Suzuki & Price, 1985),

prednisolone (Smith, 1986), and hydrocortisone (Cavalier, Benoit, & Thies, 1986). The low solubility of these therapeutic agents in the water phase resulted in their successful encapsulation within polymeric microspheres (O'Donnell & McGinity, 1997). However, this fabrication method is not useful for the encapsulation of hydrophilic agents due to their insolubility in the inner oil phase. The diffusion of water-soluble agents from the oil phase to the water phase during formulation accounts for the obtained low encapsulation efficiencies by o/w emulsion (Iqbal et al., 2015). Double emulsion method, w/o/w, plays a pivotal role in the encapsulation of hydrophilic agents. In this technique, the oil phase separates the inner water phase containing the hydrophilic drug from the outer water phase and then the precipitation of the polymer following the evaporation of the organic solvent contributes to obtaining high encapsulation efficiencies (Alex & Bodmeier, 2008).

TMZ has previously been encapsulated within PLGA microspheres with the conventional emulsification methods such as o/w and w/o/w. However, the encapsulation efficiencies reported for TMZ-loaded PLGA microspheres prepared with the aforementioned techniques have been low. The partitioning of amphiphilic TMZ into the outer water phase was accounted for obtaining poor encapsulation efficiencies (White et al., 2011). Saturation of the exterior water phase with TMZ has also been suggested to inhibit the diffusion of TMZ outwards and improve the encapsulation efficiency (White et al., 2011; H. Zhang & Gao, 2007). The fabrication of TMZ-loaded PLGA microspheres with these techniques is not cost-effective, since a considerable amount of TMZ is consumed, but is poorly encapsulated within the microspheres. Furthermore, the high IC_{50} (the concentration of drug needed for reaching 50% inhibition of cell growth *in vitro*) values of TMZ require for inducing tumour cytotoxicity, along with the low encapsulation

of TMZ within PLGA microspheres, necessitate excessive polymer contents in practice for glioblastoma cell treatment. Therefore, there is a substantial room for improving the current design of these microspheres in the treatment of GBM (White et al., 2011).

To date, there has been no published research on the fabrication of TMZ-loaded PLGA microspheres with high encapsulation efficiency. A fabrication technique capable of improving the encapsulation of TMZ within PLGA microspheres could decrease the amount of drug needed for microsphere preparation, and also address the high IC_{50} values of TMZ to glioblastoma cells without administration of high polymer contents. This chapter investigates a possible emulsification technique to encapsulate TMZ within PLGA microspheres successfully. The first aim of this chapter is preparing PLGA microspheres loaded with TMZ via oil-in-oil (o/o) emulsion. In this fabrication technique, an external oil phase in which TMZ has poor solubility was used in order to prevent the diffusion of TMZ outwards and enhance the encapsulation efficiency. The second aim of this chapter is to optimize the TMZ release kinetics from PLGA microspheres by altering the microsphere's fabrication parameters such as polymer concentration.

2.1. Materials and methods

Preparation of o/w single emulsion microspheres: PLGA microspheres were fabricated using an o/w emulsion procedure previously described by Zhang, H. and Gao, S., with a little modification (H. Zhang & Gao, 2007). 200 mg of PLGA (50:50) (Resomer RG504H) (Sigma, St. Louis, USA) was dissolved at room temperature in 16 ml of dichloromethane (Fisher Scientific) using a magnetic mixer (Thermo Scientific) for 10 minutes at a speed of 400 rpm to obtain the oil phase. 3.75 mg of temozolomide acid (Ontario Chemicals Inc., On, Canada) was dispersed into the oil phase to fabricate PLGA

microspheres loaded with TMZ. To prepare 80 ml of 2% polyvinyl alcohol (PVA) (Sigma, St. Louis, USA) solution which was used as our water phase, the required amount of PVA was dissolved in de-ionized water kept at 85°C using a magnetic mixer for 30 minutes at 850 rpm. We then emulsified our oil phase with the prepared water phase using a vortexer (Fisher Scientific) at a speed of 3000 rpm for 15 seconds. Subsequently, the prepared emulsion was kept at 35 ºC while mixing at a speed of 500 rpm for 4 hours to remove the organic solvent. The resulting microspheres were centrifuged at 4000 rpm (Eppendorf 5810R) and washed twice with de-ionized water to remove any remaining PVA. We then freeze-dried the microspheres for 24 hours. PLGA microspheres loaded with TMZ were also fabricated via the saturated water phase. We prepared those microspheres in the same manner as that of o/w emulsion. However, in this case, we saturated the 80 ml of 2% (w/v) PVA solution with adding 400 mg of TMZ before emulsification with the oil phase (Ananta et al., 2016; H. Zhang & Gao, 2007).

Preparation of w/o/w double emulsion microspheres: We made some modifications to previously developed w/o/w double emulsion technique in order to fabricate TMZ-loaded PLGA microspheres (Kashi et al., 2012). 1% (w/v) PVA solution was prepared by dissolving the required amount of PVA in de-ionized water for 30 minutes at 85°C while mixing at a speed of 850 rpm. The inner water phase was obtained by dissolving 3.75 mg of TMZ in 3 ml of 1% (w/v) PVA solution via vortex mixing for 3 minutes at 3000 rpm. This water phase was then emulsified with our oil phase which consisted of 125 mg of PLGA dissolved in 10 ml of dichloromethane. The emulsification was conducted by vortex mixing for 15 seconds at 3000 rpm. The previously made 1% (w/v) PVA solution was diluted with de-ionized water to obtain 0.5% and 0.2% (w/v) PVA

solutions. Afterward, the resulting w/o emulsion was dispersed into 12.5 ml of 0.5% (w/v) PVA solution. A vortex mixer at a speed of 3000 rpm for 20 seconds was used to obtain the w/o/w emulsion. Subsequently, the prepared emulsion was transferred into 60 ml of 0.2% (w/v) PVA solution and held at 35 ºC while mixing at 500 rpm for 4 hours to achieve the evaporation of the organic solvent. The final microspheres were isolated by centrifugation at 4000 rpm and washed three times with de-ionized water, then freeze-dried for 24 hours.

Preparation of o/o single emulsion microspheres: PLGA microspheres were prepared with o/o emulsion according to the procedure developed by Mahdavi *et al.* (Mahdavi et al., 2010). A known amount of PLGA was dissolved in 3 ml acetonitrile (Caledon Laboratories, Georgetown, On, Canada) for 10 minutes at a speed of 400 rpm to obtain the first oil phase. The required amount of PLGA was determined based on the polymer/acetonitrile ratio (w/v, %) (1.25, 5, and 10). When making TMZ-loaded PLGA microspheres, 3.75 mg of TMZ was added to the aforementioned oil phase. The second oil phase was 40 ml of viscous liquid paraffin (Caledon Laboratories, Georgetown, On, Canada) containing 200 µl of Span 80® (Sigma, St. Louis, USA). The first oil phase was emulsified by the second oil phase using a vortex mixer for 45 seconds at a speed of 3000 rpm. The resulting emulsion was continuously stirred at 55 ºC for 2 hours at a speed of 700 rpm to ensure the complete evaporation of the organic solvent. The microspheres were then collected by centrifugation at a speed of 4000 rpm and washed three times with n-hexane (Fisher Scientific) to remove any traces of liquid paraffin and Span 80®. Finally, the prepared microspheres were air dried for 48 hours to remove residual n-hexane (Kashi et al., 2012). In another study to reduce the amount of TMZ encapsulated near the surface of

PLGA microspheres and obtain lower initial burst release, we prepared microspheres with the saturation of acetonitrile with TMZ (30 mg). Since one of the reasons for initial burst release and fast overall release rate is the diffusion of the drug toward the surface of polymeric microspheres during the evaporation of the organic solvent (Yeo & Park, 2004).

Encapsulation efficiency: The extraction of TMZ from the fabricated microspheres was used to determine the encapsulation efficiency (EE). In order to measure the encapsulation efficiency of TMZ-loaded PLGA microspheres fabricated by o/w and w/o/w emulsion, accurately weighed blank and TMZ-loaded microspheres were placed into 1.5 ml Eppendorf tubes, and 300 µl of dichloromethane was added to each sample. The samples were then mixed (Eppendorf® MixMate®) for 5 minutes at a speed of 330 rpm. Afterward, 1200 µl of dichloromethane was added to each sample. The Eppendorf tubes were vortexed for 15 seconds at a speed of 3000 rpm to ensure the complete dissolution of PLGA. They were then centrifuged multiple times for 5 minutes at 15,000 rpm speed. The supernatant of each sample was collected, and the TMZ content of each supernatant was analysed by using a plate reader (Tecan Infinite® M200Pro) at λ_{max} 327 nm. The following equation was used to calculate the encapsulation efficiency of PLGA microspheres loaded with TMZ:

$$Encapsulation\ efficiency\ (\%) = \frac{TMZ_{encpasulated}}{TMZ_{theoritical}} \times 100 \quad (1)$$

Where $TMZ_{encpasulated}$ is the actual amount of TMZ in the fabricated microspheres and $TMZ_{theoritical}$ is the initial amount of TMZ used for the preparation of microspheres in mg (H. Zhang & Gao, 2007). The same procedure was used to determine the encapsulation efficiency of TMZ-loaded PLGA microspheres prepared by o/o emulsion technique. However, in this case, acetonitrile was used for dissolving PLGA.

Characterization of surface morphology and size of PLGA microspheres: A scanning electron microscopy (SEM) machine (Hitachi S-4800) was used to characterize both blank and TMZ-loaded PLGA microspheres prepared from different PLGA concentrations (1.25, 5, and 10%). After dispersing 1 mg of each type of microspheres into 1 ml of anhydrous ethanol, 10 µl of the prepared suspensions were placed on SEM stubs and air-dried. The SEM samples were then coated with gold-palladium using a sputter coater (Anatech Hummer VI) to improve the surface conductivity. An accelerating voltage of 1.0 kV and working distances of 8.3, 8.4, 8.5, and 8.6 mm were used for taking the SEM images. Commercially available ImageJ software was used to analyse the SEM images and thus determining the diameter of microspheres.

***In vitro* release study of TMZ:** 4 mg of microspheres were suspended in 1 ml of tris buffer (pH 6.86) (Sigma, St. Louis, USA) in an Eppendorf tube. TMZ is more stable in the acidic pH, so tris buffer with the pH of 6.86 was used to carry out the release studies (Rottenberg et al., 1985). The Eppendorf tubes were then incubated at 37°C. At specific time intervals, Eppendorf tubes were taken out from the incubator and centrifuged at a speed of 15,000 rpm for 10 minutes. The whole medium was then collected and replaced with the fresh release medium. A plate reader at λ_{max} 327 nm was used to analyse the withdrawn supernatant. Previously, a series of TMZ solutions (dissolved in tris buffer) with known concentrations were analysed with a plate reader at λ_{max} 327 nm to prepare a standard curve which could relate the absorbance (x-axis) to the concentration (y-axis). The following standard equation was derived based on the fitted curve (Figure 13):

$$y = 151.28x + 0.2535 \quad (2)$$

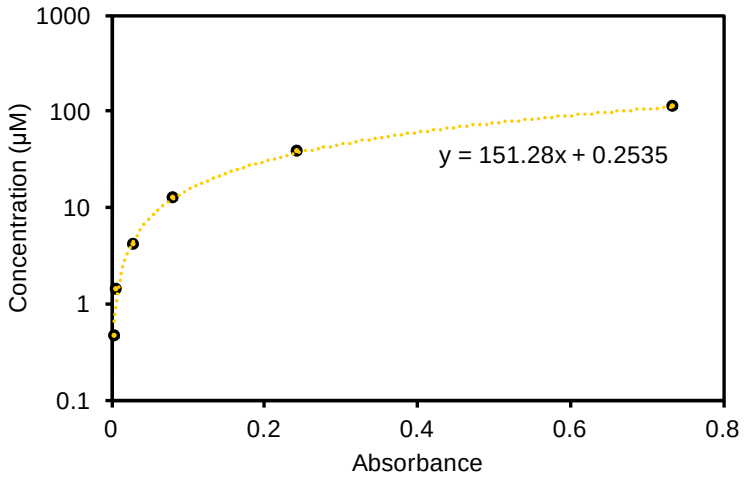

Figure 13. Standard curve correlates the absorbance to the concentration of TMZ. Error bars are the SD (n=3).

After correlating the absorbance of each release supernatant to TMZ concentration using the standard equation, we used the following equation to find out the TMZ release percentage at the predetermined time point:

$$Release\ (\%) = \frac{C * V}{M_{ms} * D * EE} \times 100 \quad (3)$$

Where C is the concentration of TMZ in mg/ml, V is the volume of media in ml, M_{ms} is the amount of microsphere placed in each Eppendorf tube in mg, D is TMZ percentage, and EE is the encapsulation efficiency.

2.2. Results and discussion

PLGA microspheres loaded with TMZ fabricated via different methods and parameters were characterized regarding their encapsulation efficiency. Table 3 shows the effect of four different fabrication procedures on the encapsulation efficiency of polymeric microspheres. Low encapsulation efficiencies of 0.87 ± 0.52% and 1.34 ± 0.03% were obtained for TMZ-loaded PLGA microspheres prepared with o/w and w/o/w emulsion, respectively. The partitioning of amphiphilic TMZ from the inner phase to the outer water

phase during the evaporation of the organic solvent was the main reason for achieving low encapsulation efficiencies. A similar trend was previously reported by Ananta *et al.* (Ananta et al., 2016). TMZ-loaded PLGA microspheres prepared via the saturation of outer water phase with TMZ before the emulsification process also showed the poor encapsulation efficiency of 5.50 ± 1.18%. We believed that washing the microspheres with de-ionized water resulted in removing a considerable amount of TMZ which was encapsulated close to the surface of microspheres in this preparation method (near to the interface of the inner oil and outer water phase). We hypothesized that using an external phase in which TMZ has poor solubility could prevent the diffusion of TMZ outwards and result in enhancing the encapsulation efficiency. TMZ-loaded PLGA microspheres prepared with the same amount of TMZ and PLGA concentration by using o/o emulsion showed encapsulation efficiencies as high as 48.30 ± 6.20% because of the poor solubility of TMZ in the outer phase (liquid paraffin). Moreover, increasing the PLGA concentration from 1.25% to 10% demonstrated an increase in the encapsulation efficiency from 48.30 ± 6.20% to 61.15 ± 6.80%. We believed that the high viscosity of concentrated PLGA solution slows down the partitioning of TMZ into the exterior phase. A similar trend was demonstrated by Yeo, Y. and Park, K. (Yeo & Park, 2004).

Table 3. Encapsulation efficiency of PLGA microspheres loaded with TMZ prepared with different emulsion methods.

Fabrication method	PLGA concentration (w/v, %)	Encapsulation efficiency (%)
o/w	1.25	0.87 ± 0.52
o/w with saturation	1.25	5.50 ± 1.18
w/o/w	1.25	1.34 ± 0.03

o/o	1.25	48.30 ± 6.20
o/o	5	58.03 ± 2.60
o/o	10	61.15 ± 6.80

Both blank and TMZ-loaded PLGA microspheres fabricated with different PLGA concentrations via o/o emulsion were imaged with SEM to determine their morphology and size distribution. SEM images revealed that both blank and loaded microspheres have a spherical shape with smooth surfaces (Figure 14).

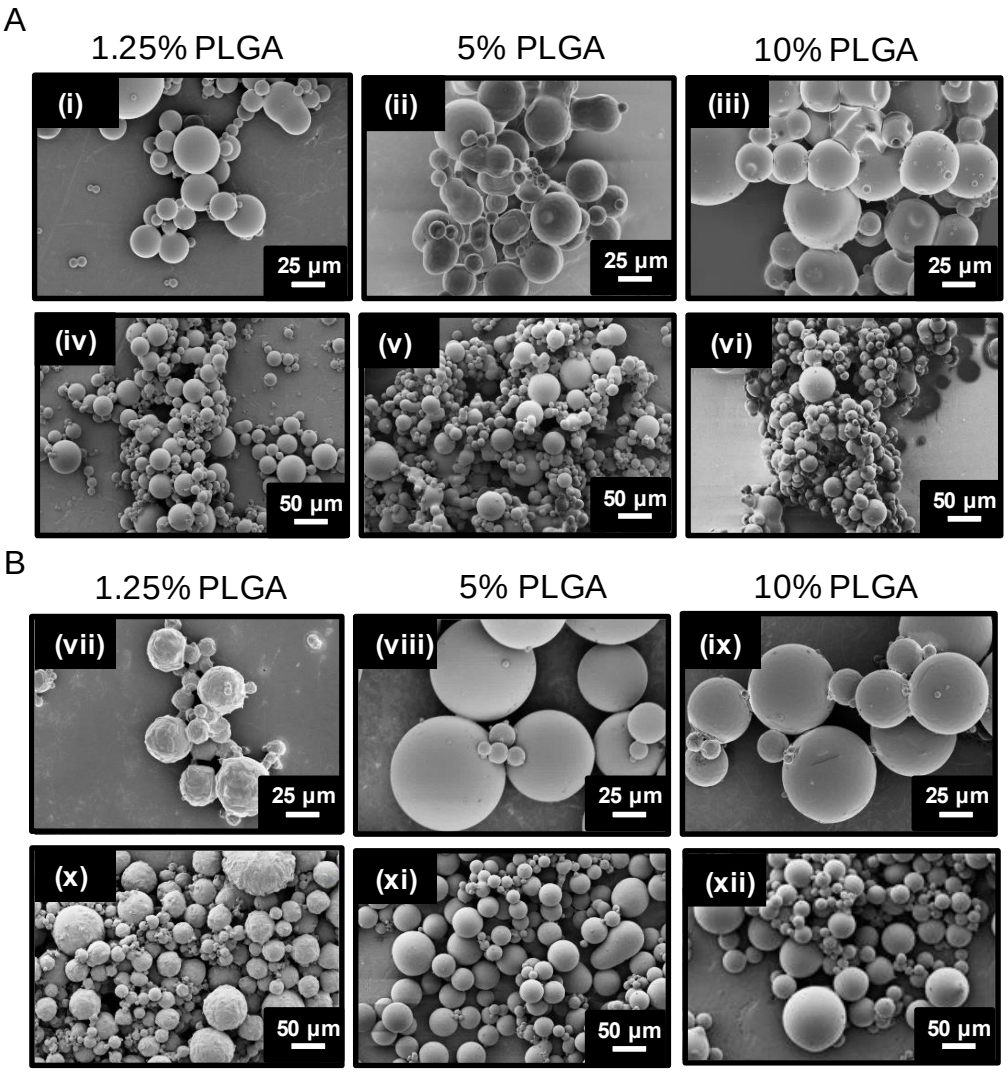

Figure 14. SEM images of (A) blank and (B) TMZ-loaded PLGA microspheres prepared from different PLGA concentrations (1.25, 5, and 10%). SEM images were taken at (i) X800, (ii) X800, (iii) X800, (iv) X200, (v) X200, (vi) X200, (vii) X800, (viii) X800, (ix) X800, (x) X200, (xi) X200, (xii) X200 magnification.

The analysis of SEM images showed that the diameter of the PLGA microspheres was not uniform (Figure 15).

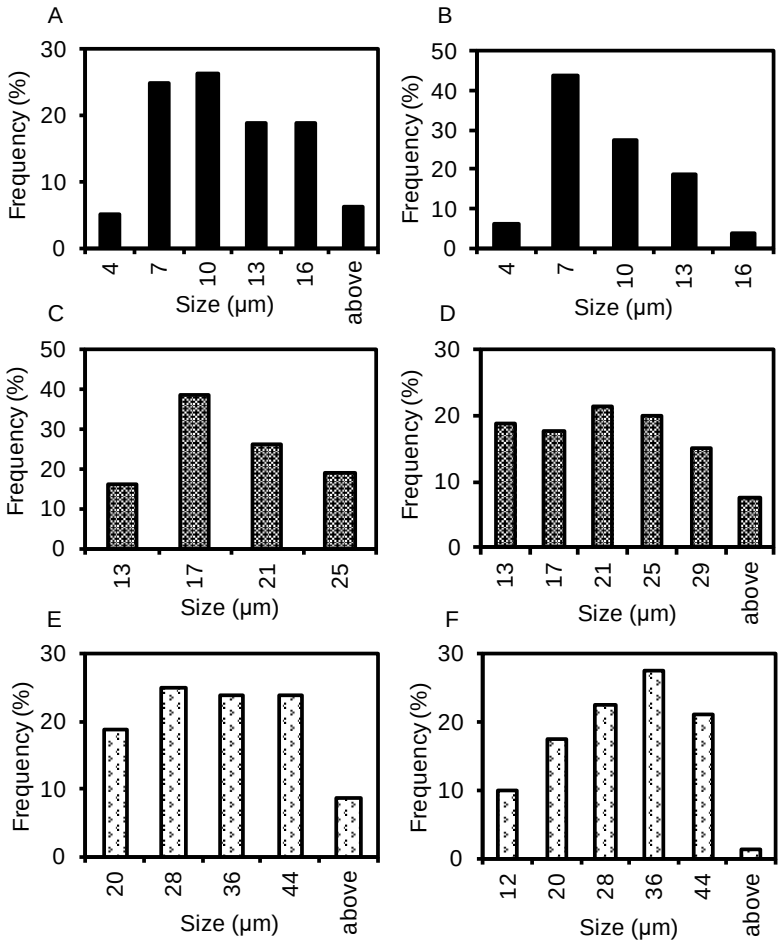

Figure 15. Size distribution of blank and TMZ-loaded PLGA microspheres prepared with (A, B) 1.25% PLGA concentration, (C, D) 5% PLGA concentration, (E, F) 10% PLGA concentration. Measurements were taken with the commercially available ImageJ software.

SEM images' analysis also demonstrated that with the same concentration of PLGA, no considerable difference in the average size was observed between blank and loaded microspheres. As shown in Figure 16, an increase in PLGA concentration from 1.25% to 10% resulted in an increase in the average size from 9.83 ± 3.91 µm to 30.29 ± 9.71 µm for blank microspheres. The same trend was observed for TMZ-loaded PLGA microspheres, with an increase from 7.61± 2.74 µm to 27.15 ± 10.04 µm for 1.25% and 10% PLGA concentration, respectively. Mahdavi *et al.* previously reported a similar trend (Mahdavi et al., 2010). Increase in PLGA concentration contributes to obtaining a more

viscous polymer solution which, in turn, results in the preparation of microspheres with a larger size.

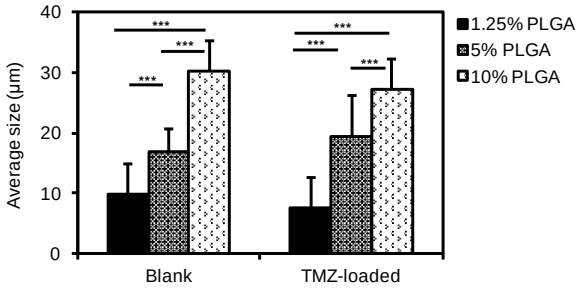

PLGA concentration (w/v, %)	Average size (µm)	
	Blank	TMZ-loaded
1.25	9.83 ± 3.91	7.61 ± 2.74
5	16.82 ± 3.75	19.53 ± 6.66
10	30.29 ± 9.71	27.15 ± 10.04

Figure 16. The average size of blank and TMZ-loaded PLGA microspheres fabricated with different PLGA concentrations. The average size of blank and TMZ-loaded PLGA microspheres fabricated with 1.25%, 5%, and 10% PLGA concentration is 9.83 ± 3.91 µm, 7.61 ± 2.74 µm, 16.82 ± 3.75 µm, 19.53 ± 6.66 µm, 30.29 ± 9.71 µm, and 27.15 ± 10.04 µm, respectively. Error bars are the SD. *** P<0.0005.

By altering the size of drug-loaded PLGA microspheres, one can simply influence the release kinetics of encapsulated drug. It has been reported by Vert *et al.* that the hydrolytic degradation of microspheres depends on their size. They demonstrated that large-sized microspheres undergo heterogeneous degradation which means that the rate of degradation at the core of microspheres is higher than that of the surface. However, microspheres with a smaller size (smaller than 300 µm) have a slower, homogenous degradation (Grizzi, Garreau, Li, & Vert, 1995; Vert, Mauduit, & Li, 1994). The size range investigated in the current work suggested that the degradation rate does not play a significant role in optimizing the release kinetics of our microspheres. However, changing the size of microspheres can affect the release rate of TMZ as a diffusion-based phenomenon. As stated previously, increasing PLGA concentration from 1.25% to 10% increased the average size of microspheres which, in turn, affects the surface-area-to-volume ratio of fabricated microspheres. *In vitro* release studies demonstrated that TMZ-loaded PLGA microspheres fabricated by 1.25% PLGA concentration have an initial burst

release of 93% during the first 24 hours and a fast overall release rate (Figure 17). The initial burst release reduced considerably, and the overall release rate became prolonged when microspheres were prepared with higher polymer concentration due to their smaller surface-area-to-volume ratio. TMZ-loaded PLGA microspheres fabricated by 5% and 10% PLGA concentration showed an initial burst release of 48% and 27%, respectively. Additionally, the aforementioned microspheres could provide an extended TMZ release up to 16 and 20 days, respectively.

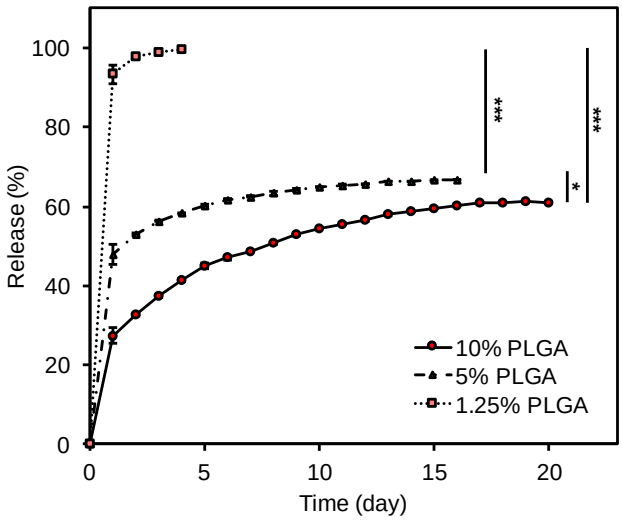

Figure 17. *In vitro* TMZ release from PLGA microspheres fabricated with different PLGA concentrations (1.25, 5, and 10%). A slower release rate was obtained by increasing the polymer concentration. Error bars are the SD (n=3). * P<0.05, and *** P<0.0005.

As described previously, we hypothesized that the saturation of organic solvent with TMZ could reduce the diffusion of the drug to the surface of PLGA microspheres during the evaporation of acetonitrile, and subsequently decrease the initial burst release. However, TMZ-loaded PLGA microspheres fabricated with the saturation of acetonitrile with TMZ showed an initial burst release of 99% (Figure 18).

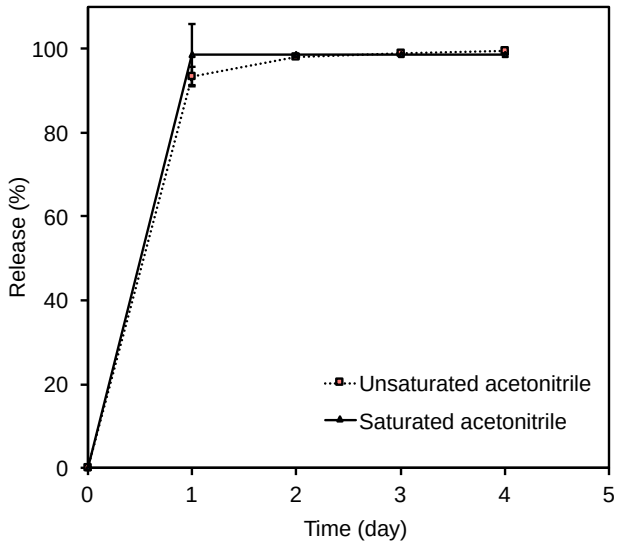

Figure 18. ***In vitro*** **TMZ release from PLGA microspheres fabricated with different amount of TMZ (3.75 mg and 30 mg). Amount of TMZ dissolved in acetonitrile did not show any effect on the initial burst release. Error bars are the SD (n=3).**

2.3. Conclusion

TMZ-loaded PLGA microspheres, one of the main components of GlioMesh, were prepared using o/o emulsion solvent evaporation technique. This method of fabrication allows for obtaining high encapsulation efficiencies due to the low solubility of amphiphilic TMZ in, liquid paraffin, the outer phase. Therefore, the proposed technique of preparation is more cost-effective compared to the conventional fabrication methods (o/w and w/o/w) which consume a great amount of drug, while resulting in low encapsulation efficiencies. Additionally, our TMZ-loaded microspheres allow for addressing the high IC_{50} values indicated by human glioblastoma cells for TMZ without administration of excessive polymer contents. The release kinetics of TMZ from PLGA microspheres were also optimized by altering the polymer concentration used in the fabrication process.

Chapter 3: Fabrication of GlioMesh

Microsphere-loaded hydrogels have been reported as a promising approach to locally deliver therapeutic agents to the desired site in the body over an extended period (DeFail, Chu, Izzo, & Marra, 2006; Duvvuri, Janoria, & Mitra, 2005; Fattal, De Rosa, & Bochot, 2004; Ungaro et al., 2006). Embedding polymeric microspheres within hydrogels allows the microspheres to be immobilized around the desired area. Lee, J. and Lee, K.Y. developed an injectable alginate hydrogel that incorporated with PLGA microspheres for localized protein delivery (Figure 19). They believed this combination system could address the limitations of each carrier including the large initial burst release of bovine serum albumin (BSA) from the hydrogel and the continuous microspheres removal by macrophages (J. Lee & Lee, 2009).

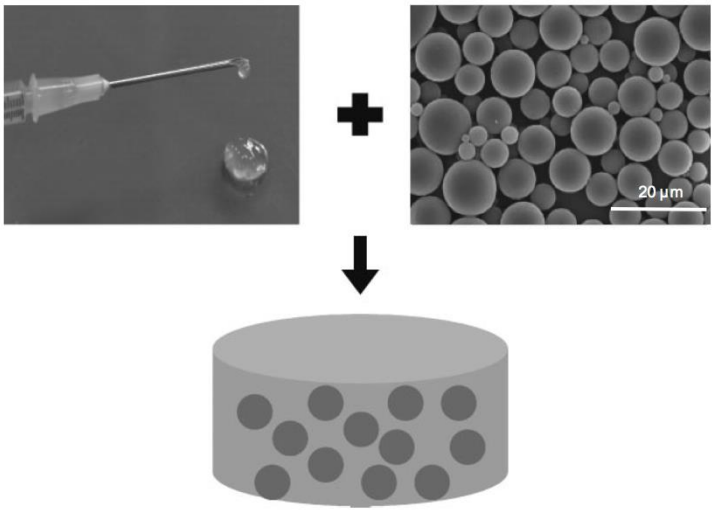

Figure 19. Embedment of PLGA microspheres into disks made of alginate hydrogel. Reproduced with permission (J. Lee & Lee, 2009).

In another study, Defail *et al.* designed a microsphere-loaded poly (ethylene glycol) (PEG)-based hydrogel for cartilage tissue engineering application (DeFail et al., 2006). They first encapsulated transforming growth factor-β1 (TGF-β1) into PLGA microspheres and then

embedded these microspheres into the biodegradable hydrogel which provided the advantage of obtaining a more sustained release profile compared with naked microspheres (DeFail et al., 2006). The diffusive behaviour of microsphere-loaded hydrogels, which is an essential factor in determining the release kinetics of drug, depends on the surface-area-to-volume ratio of the structure. Incorporation of polymeric microspheres within a 3D bioprinted hydrogel-based mesh allows for easily adjusting this characteristic. The capability of 3D bioprinting to alter the fibre diameter through printing with different print head pressures and printing speeds results in tuning of the surface-area-to-volume ratio of 3D constructs.

The first ever 3D printing technology, stereolithography, was developed by Charles W. Hull in 1986 (Kalaskar, 2017; Murphy & Atala, 2014). 3D printing is the layer-by-layer deposition of materials for fabrication of a 3D structure, and for this reason it is also known as additive manufacturing (Pedde et al., 2017). In this method of fabrication 3D models created by computer-aided-design (CAD) are transcribed to codes, allowing for precise, computer control over spatial movement and material deposition. This technology has received a great deal of attention in different engineering and biomedical fields (Bandyopadhyay, Bose, & Das, 2015). The main technologies used for 3D bioprinting are inkjet, microextrusion, and laser-assisted printing (Kalaskar, 2017). Continuous disposition of fibre-based constructs on the printer's bed by using microextrusion techniques facilitates the extrusion of biomaterials with a broader range of viscosity (Murphy & Atala, 2014; Pedde et al., 2017). This characteristic of the microextrusion method accommodates a greater range of materials and allows for the bioprinting of pastes and hydrogels with high concentration of hydrophilic polymers (Luo, Lode, & Gelinsky, 2013). In this fabrication

technique, simultaneous or post extrusion crosslinking results in high shape fidelity after printing (Pedde et al., 2017).

Alginate is a well-known biopolymer extracted from brown seaweed and has been commonly used for wound dressing, drug delivery, and tissue engineering applications because of its biocompatibility, low toxicity, non-immunogenicity, relatively low cost, and ease of gelation (Akbari et al., 2014; K. Y. Lee & Yuk, 2007). Combining the aqueous solution of alginate with ionic crosslinking agents such as divalent calcium ions is one of the most commonly used techniques for the preparation of alginate hydrogel (Figure 20). This immediate sol-gel transition of alginate allows for its successful use in 3D bioprinting (Akbari et al., 2016; Kalaskar, 2017).

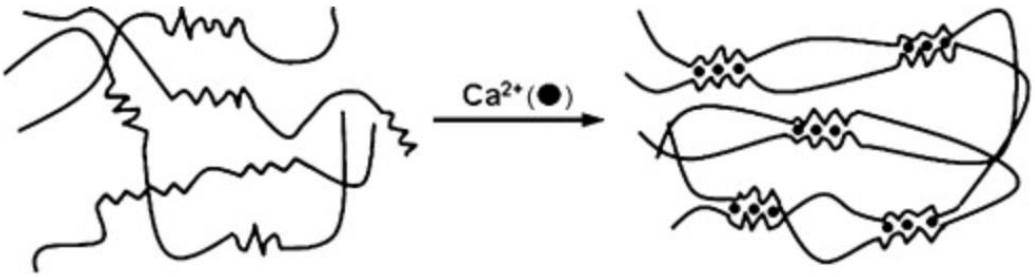

Figure 20. Alginate hydrogel formation by ionic crosslinking (egg-box model). Reproduced with permission (Yong & Mooney, 2012).

As described previously the embedment of polymeric microspheres within a 3D bioprinted hydrogel-based mesh offers numerous advantages including the inhibition of unwanted migration of microspheres away from the tumour site, and obtaining a more sustained release of the therapeutic agent. The first aim of this chapter is to demonstrate the use of a microextrusion system to fabricate a 3D bioprinted alginate mesh incorporated with TMZ-loaded PLGA microspheres (GlioMesh). The second aim is to characterize the 3D bioprinted meshes in terms of their fibre diameter and surface-area-to-volume ratio.

The last goal is to evaluate the functionality of GlioMesh by conducting *in vitro* cell viability tests on U87 human glioblastoma cell line.

3.1. Materials and methods

Fabrication and characterization of GlioMesh: A previously developed microextrusion technique by Lou *et al.* was used for fabrication of GlioMesh (Luo et al., 2013). In this approach, a 3D bioprinter (CELLINK +, Gothenburg, Sweden) was used to create both blank and microsphere-loaded meshes. We used a single-needle extrusion system to print alginate solution with relatively high concentration (16%w/v) (Figure 21). The considerably high viscosity of this solution contributed to maintaining the structural integrity of the 3D bioprinted mesh.

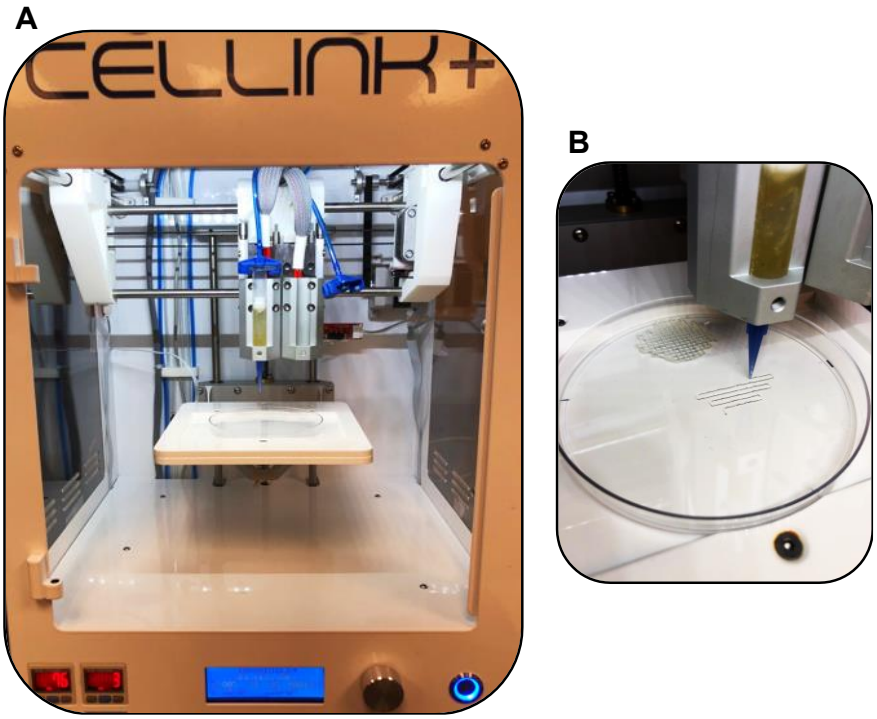

Figure 21. Photographic images of (A) commercial 3D bioprinter, CELLINK, and (B) single-needle extrusion system used for fabrication of both blank and microsphere-loaded meshes.

The proper amount of TMZ-loaded PLGA microspheres-determined by the desired TMZ content in the final mesh-was added into 5 ml of de-ionized water and vortexed for 1

minute. We then added sodium alginate (Sigma, St. Louis, USA) to the previous solution in order to obtain a total alginate concentration of 16% (w/v). The prepared mixture was stirred manually using a glass bar to get a uniform paste. We transferred this bioink into the cartridge of the 3D bioprinter and printed with the printing speed ranging from 250 mm/min to 450 mm/min and print head pressure between 40 kPa to 120 kPa. The 3D bioprinted microsphere-loaded mesh was then crosslinked by adding 4% (w/v) $CaCl_2$ (Bio Basic Inc., Toronto, Canada) solution on top. We printed blank meshes with the same procedure without adding microspheres to the alginate solution. A light microscope (Zeiss Axio Observer, Oberkochen, Germany) was used to observe meshes printed with different printing speeds, print head pressures, and microsphere concentrations and the commercially available ImageJ software was used to measure the diameter of individual fibres.

Fabrication of alginate fibres by using wetspinning technique: Wetspinning, which relies on the injection of a pre-polymer solution into a coagulation bath, was used to fabricate both blank and TMZ-releasing alginate fibres (Tamayol et al., 2013). Microsphere-loaded and blank alginate solutions were prepared by the same procedure described for the fabrication of 3D bioprinted meshes. The prepared pastes were then loaded into 3 ml plastic syringes (Terumo, Japan). Afterward, we used a syringe pump (Harvard Apparatus) to pump the pastes at an infusion rate of 500 µl/min into a 4% (w/v) $CaCl_2$ coagulation bath. Displacement of divalent calcium ions of $CaCl_2$ with monovalent sodium ions within sodium alginate results in ionic crosslinking of fibres. Two different hypodermic needles, 18 and 21 gauge, were used to fabricate fibres with a diameter in the range of the 3D bioprinted meshes' diameter in our wetspinning process.

***In vitro* release study of TMZ:** After washing the wetspun fibres with de-ionized water, blank and microsphere-loaded alginate fibres were placed into dialysis tubing (Fisher Scientific) containing 1.5 ml of tris buffer. The dialysis tubing was then transferred into a Falcon tube containing another 4.5 ml of tris buffer. The samples were then incubated at 37°C. At predetermined time intervals, the falcon tubes were removed from the incubator, and the entire medium of each sample was withdrawn and replaced with fresh media. After analysing the withdrawn supernatant with a plate reader at λ_{max} 327 nm, the release percentage of TMZ was calculated in the same way described in chapter two.

Cell culture: U87 human glioblastoma cell line was kindly given by Dr. Saeid Ghavami, from the University of Manitoba. These cells were cultured in T-25 (25 cm^2) plastic flasks (Sigma, St. Louis, USA) and incubated at 37ºC with 95% relative humidity and 5% CO_2. Dulbecco's modified Eagle medium (DMEM) (Thermo Fisher Scientific) supplemented with 10% fetal bovine serum (FBS) (Thermo Fisher Scientific), 1% penicillin (Life Technologies, Inc.) /streptomycin (Life Technologies, Inc.), and 4 µg/ml puromycin (Sigma, St. Louis, USA) was used as the cell culture media and changed every other day. We passaged the cells at 2- to 3-days intervals by using EDTA solution to remove the cells from the flask.

Cell treatment and cell viability assay: Cytotoxic effects of free TMZ, blank, and microsphere-loaded meshes were assessed in U87 glioblastoma cells. Cells were seeded at a density of 5,000 cells per well in a 96 well plate (Thermo Fisher Scientific) to evaluate the cytotoxicity of free TMZ. After 24 hours incubation, the cell culture medium was discarded and replaced with 200 µl of fresh cell culture medium containing different TMZ concentrations (100, 500, and 1000 µM). In the case of treatment with GlioMesh, a 24 well

plate (Thermo Fisher Scientific) was seeded at 25,000 cells per well density. For GlioMesh cell viability experiments, 14 mg of microspheres with TMZ loading of 100 µg/mg TMZ/PLGA were suspended in 1 ml alginate solution to obtain the TMZ concentration of 100 µM after 72 hours. 3D bioprinting of blank and microsphere-loaded meshes was carried out according to the procedure described previously. Blank and microsphere-loaded meshes were then washed with sterile water containing penicillin/streptomycin and sterilized by using UV irradiation. We placed the meshes into cell culture inserts (Millipore Sigma, St. Louis, MO, USA) and transferred them into the wells 24 hours post-seeding. To determine the proliferation and cytotoxicity of U87 glioblastoma cells, a presto blue cell viability assay was conducted. This assay relies on the reduction of resazurin (a non-fluorescent compound) in the presto blue solution into resorufin (a fluorescent compound) by metabolically active cells. At specific time intervals, after taking out the media and cell culture inserts from the seeded wells, presto blue reagent (Thermo Fisher Scientific) at a 1:9 ratio with fresh cell culture media was added to each well. Following an hour incubation period, the fluorescent intensity of the media containing presto blue withdrawn from the wells was measured at excitation wavelength of 535 nm and emission wavelength of 615 nm using a plate reader. We washed the wells of seeded plates with Dulbecco's phosphate buffered saline (DPBS) (Sigma, St. Louis, USA) and returned the cell culture media and cell culture inserts to the well plates. We used the following equation to calculate the cell viability:

$$Cell\ viability\ (\%) = \frac{absorbance\ of\ treated\ cells}{absorbance\ of\ control\ cells} \times 100 \quad (4)$$

In all experiments, six wells of each plate were used as the control without treatment. Phase contrast images of the cells were obtained at specific time points using a light microscope at 10X magnification.

3.2. Results and discussion

The porosity provided by the 3D constructs made possible by a 3D bioprinter allows for the transport of oxygen and nutrients to the tissue after implantation of GlioMesh. Additionally, the main component of bioink in this 3D bioprinting method is alginate, giving considerable flexibility to 3D structures. The flexible characteristics of GlioMesh allow for conformal contact with irregularly shaped tissue which then contributes to high doses and uniform distribution of TMZ (Figure 22).

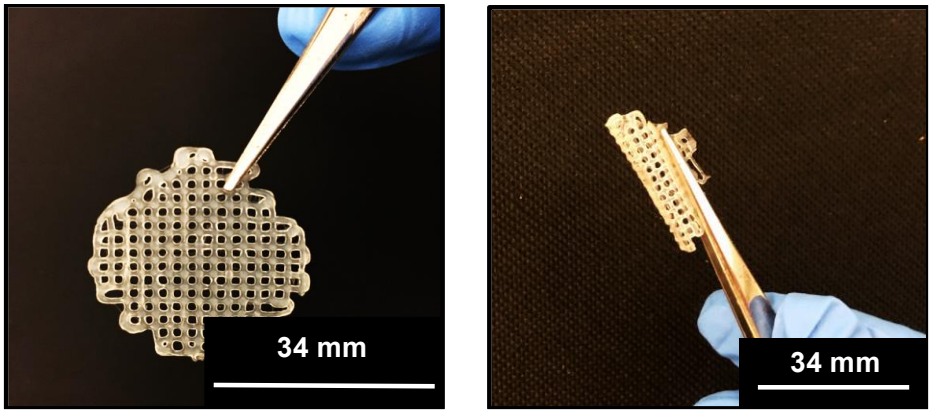

Figure 22. Photographic images of GlioMesh showing its porous (left) and flexible (right) structure.

Microextrusion 3D bioprinting technique makes it possible to adjust the fibre diameter by altering the print head pressure and the printing speed. GlioMeshes printed with different print head pressures, printing speeds, and microsphere concentrations were characterized regarding their fibre diameter. As shown in Figure 23, the variation of print head pressure from 40 kPa to 120 kPa led to a change in fibre diameter from 368 µm to 1243 µm. Deposition of more bioink from the print head was considered as the reason for the increase in fibre diameter.

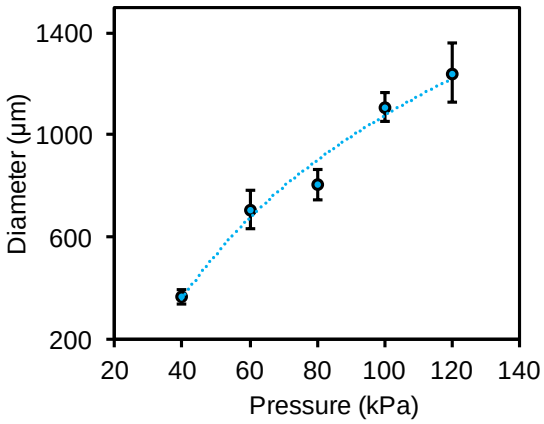

Figure 23. The effect of print head pressure on fibre diameter, printing speed kept constant (400 mm/min). Higher print head pressures contributed to increasing the fibre diameter of the 3D structure. Error bars are SD (n=6).

Microscopic images of alginate mesh printed with different pressures on the nozzle of 3D bioprinter are shown in Figure 24.

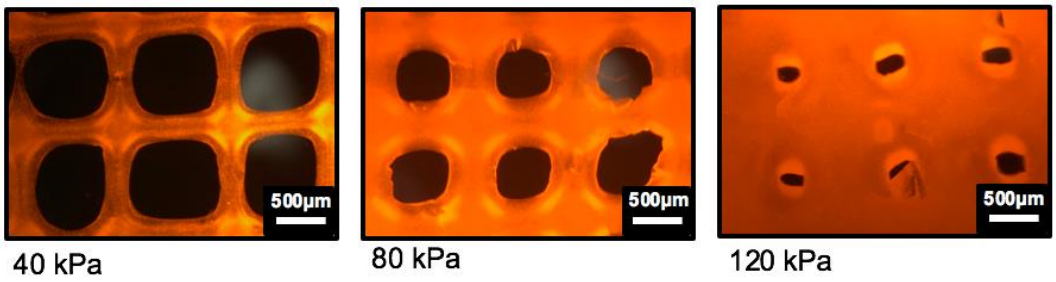

Figure 24. Microscopic images of alginate mesh printed with various pressures (40, 80, and 120 kPa).

In contrast, our results demonstrated that the diameter of fabricated fibres decreased from 1150 µm to 760 µm when we increased the printing speed from 250 mm/min to 450 mm/min because less bioink was deposited per unit length of fibres (Figure 25).

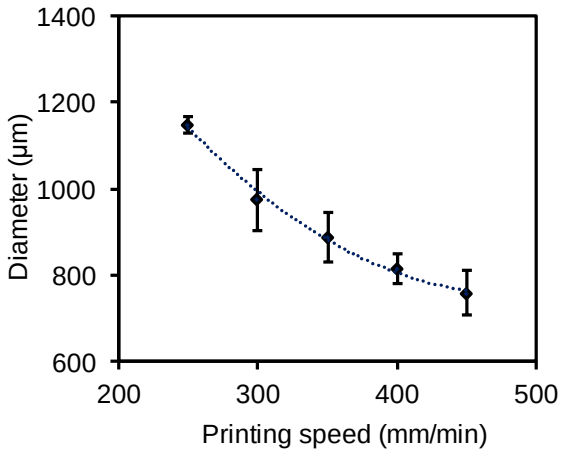

Figure 25. The effect of printing speed on fibre diameter, print head pressure kept constant (80 kPa). Higher printing speeds resulted in smaller fibre diameter. Error bars are SD (n=6).

Figure 26 shows the microscopic images of alginate mesh printed with 250, 350, and 450 mm/min printing speeds.

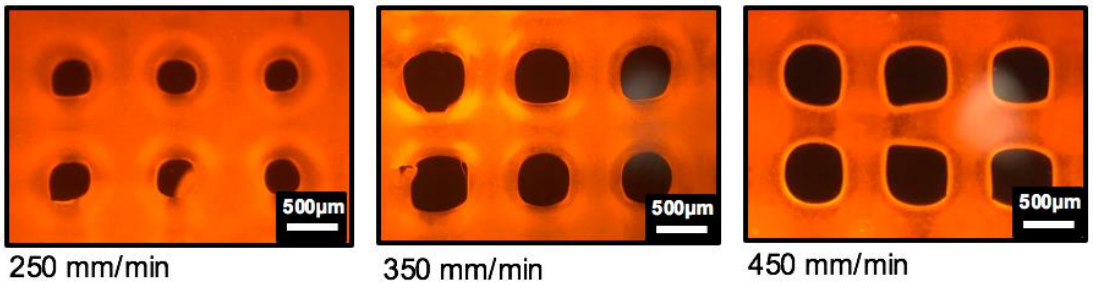

Figure 26. Microscopic images of alginate mesh printed with different printing speeds (250, 350, and 450 mm/min).

It was also shown that the microsphere concentration used for the preparation of meshes has an impact on the fibre diameter. The density of microspheres loaded onto GlioMesh demonstrated a similar effect as print head pressure on the fibre diameter. It was observed that increasing the microsphere concentration from 1 mg/ml to 6 mg/ml resulted in 347 µm increase in the diameter of fabricated fibres (Figure 27).

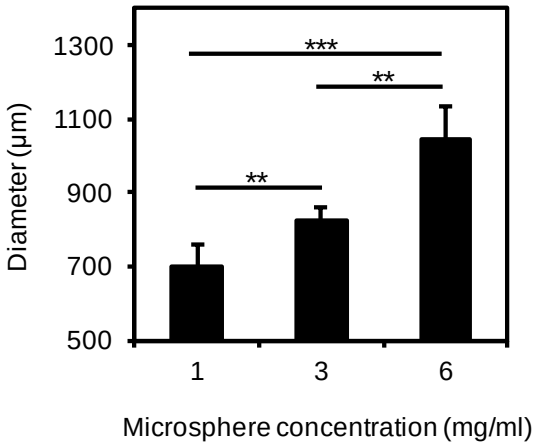

Figure 27. The effect of microsphere density on fibre diameter. The diameter of fibres increased by using higher microsphere concentrations. Error bars are SD (n=6). ** P<0.005, and *** P<0.0005.

Microscopic images of 3D bioprinted mesh fabricated with different microsphere concentrations (1, 3, and 6 mg/ml) are shown in Figure 28.

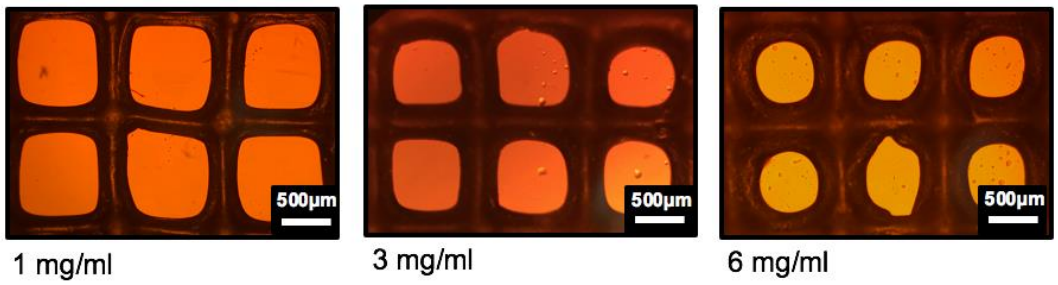

Figure 28. Microscopic images of alginate mesh prepared with various microsphere densities (1, 3, and 6 mg/ml).

Based on the following equation, the fibre diameter (D) is inversely proportional to the surface-area-to-volume ratio of 3D structures:

$$\frac{Surface\ area}{Volume} = \frac{4}{D} \quad (5)$$

The significance of the surface-area-to-volume ratio of 3D constructs lies in its substantial effect on the TMZ release kinetics as a diffusion-based phenomenon. In general, higher surface-area-to-volume ratio contributes to higher diffuse flux and thus faster drug release rate. A 70% reduction in the surface-area-to-volume ratio of 3D bioprinted meshes was

demonstrated when the print head pressure was increased from 40 kPa to 120 kPa. On the other hand, increasing the printing speed from 250 mm/min to 450 mm/min resulted in 51% increase in the surface-area-to-volume ratio of 3D constructs (Figure 29).

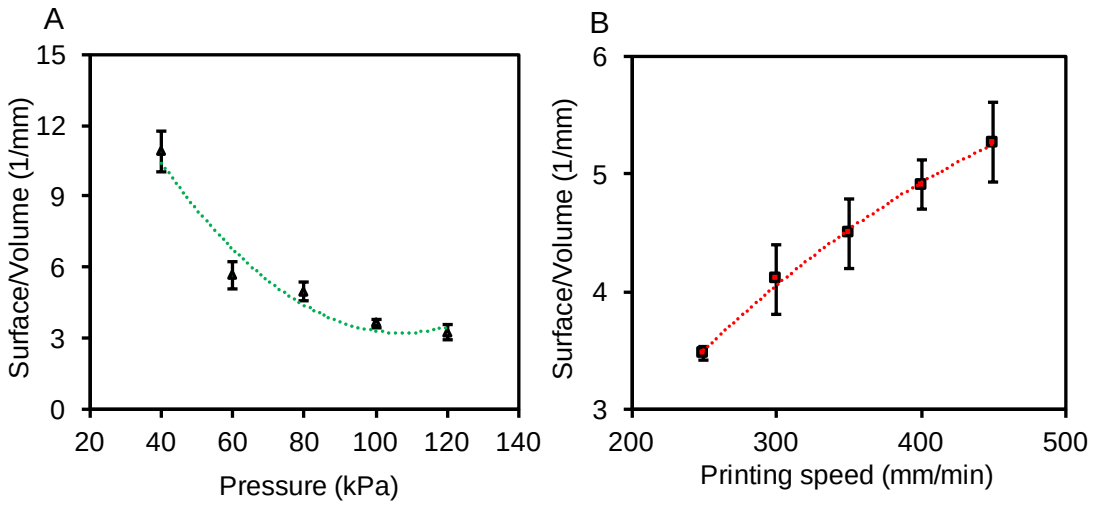

Figure 29. The effect of print head pressure (A) and printing speed (B) on the surface-area-to-volume ratio of 3D constructs. Increasing the pressure reduces the surface-area-to-volume ratio, whereas increasing the printing speed increases the surface-area-to-volume ratio. Error bars are SD (n=6).

The effect of incorporation of TMZ-loaded PLGA microspheres within alginate mesh on the TMZ release kinetics was investigated by conducting an *in vitro* release study of microsphere-loaded wet spun alginate fibres. The embedment of TMZ-loaded PLGA microspheres (fabricated with 5% PLGA concentration) within alginate fibres led to a 39% decrease in the initial burst release of TMZ and created a prolonged TMZ release up to 50 days because alginate acts as a second barrier against the drug diffusion (Figure 30).

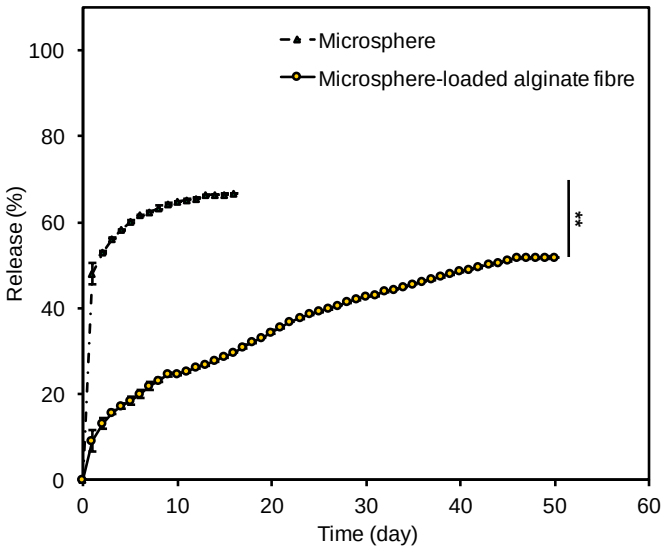

Figure 30. The effect of incorporation of TMZ-loaded PLGA microspheres within alginate fibres on the release kinetics. The embedment of microspheres prepared with 5% PLGA concentration within alginate fibres resulted in slowing down the release kinetics. Error bars are SD (n=3). ** P<0.005.

To investigate the impact of the surface-area-to-volume ratio on the TMZ release rate, we conducted the release study of microsphere-loaded alginate fibres with two different diameters. Our studies indicated that increasing the diameter of wet spun fibres from 648 µm to 1210 µm led to a slower overall TMZ release kinetic because of the smaller surface-area-to-volume ratio of thicker fibres (Figure 31).

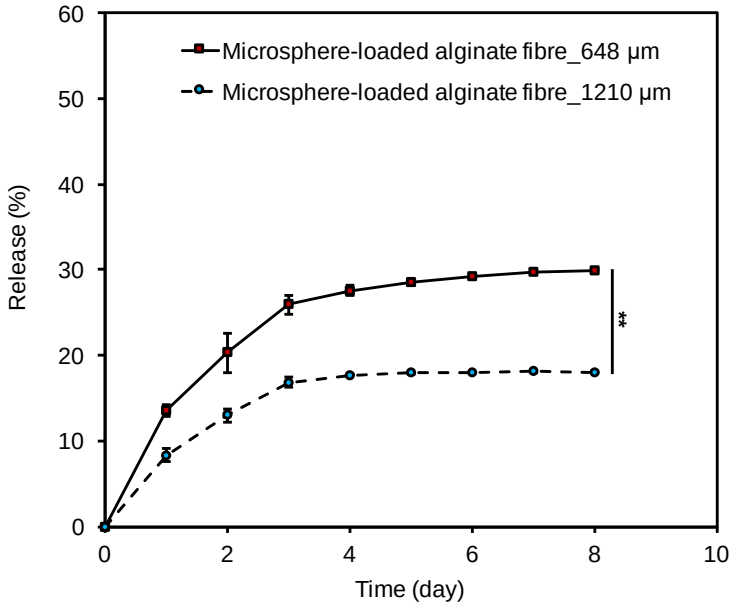

Figure 31. The effect of fibre diameter on the TMZ release rate from microsphere-loaded alginate fibres (microspheres fabricated with 1.25% PLGA concentration). Thinner alginate fibres showed a faster TMZ release rate due to their higher surface-area-to-volume ratio. Error bars are SD (n=3). ** P<0.005.

We evaluated the functionality of GlioMesh in terms of inducing cytotoxic effects by conducting *in vitro* cell viability tests on human glioblastoma cell line, U87. These cells were treated with free TMZ, blank, and microsphere-loaded meshes. Dose-dependent levels of cytotoxicity were observed when U87 cells were treated with different TMZ concentrations (100, 500, and 1000 µM). As shown in Figure 32, increasing the TMZ concentration from 100 to 1000 µM resulted in 78% and 95% reduction in the cell viability, respectively, after 96 hours treatment.

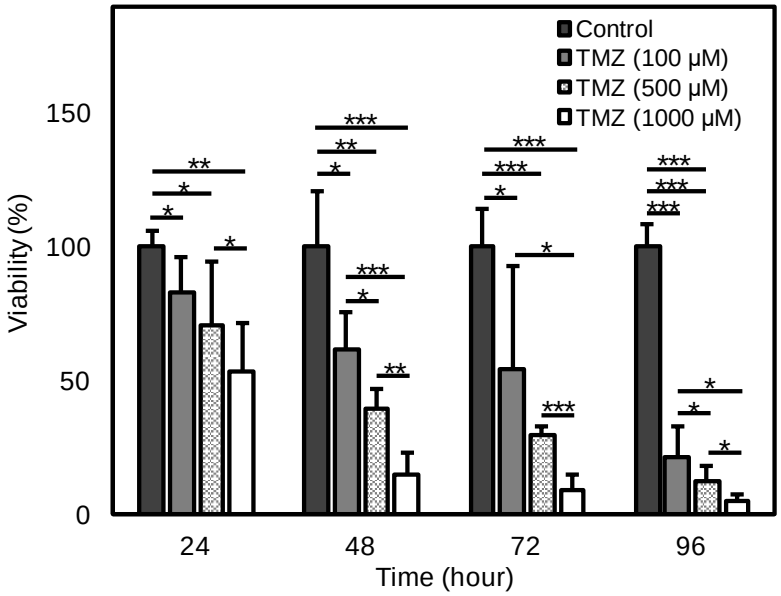

Figure 32. Cytotoxicity of different concentrations of free TMZ (100, 500, and 1000 µM) to U87 glioblastoma cells *in vitro*. Cytotoxic activity increased by increasing the free drug concentration. Error bars are SD (n=6). * P<0.05, ** P<0.005, and *** P<0.0005.

The microscopic images of U87 cells treated with various concentrations of TMZ at different time points (24, 48, 72, and 96 hours) are shown in Figure 33.

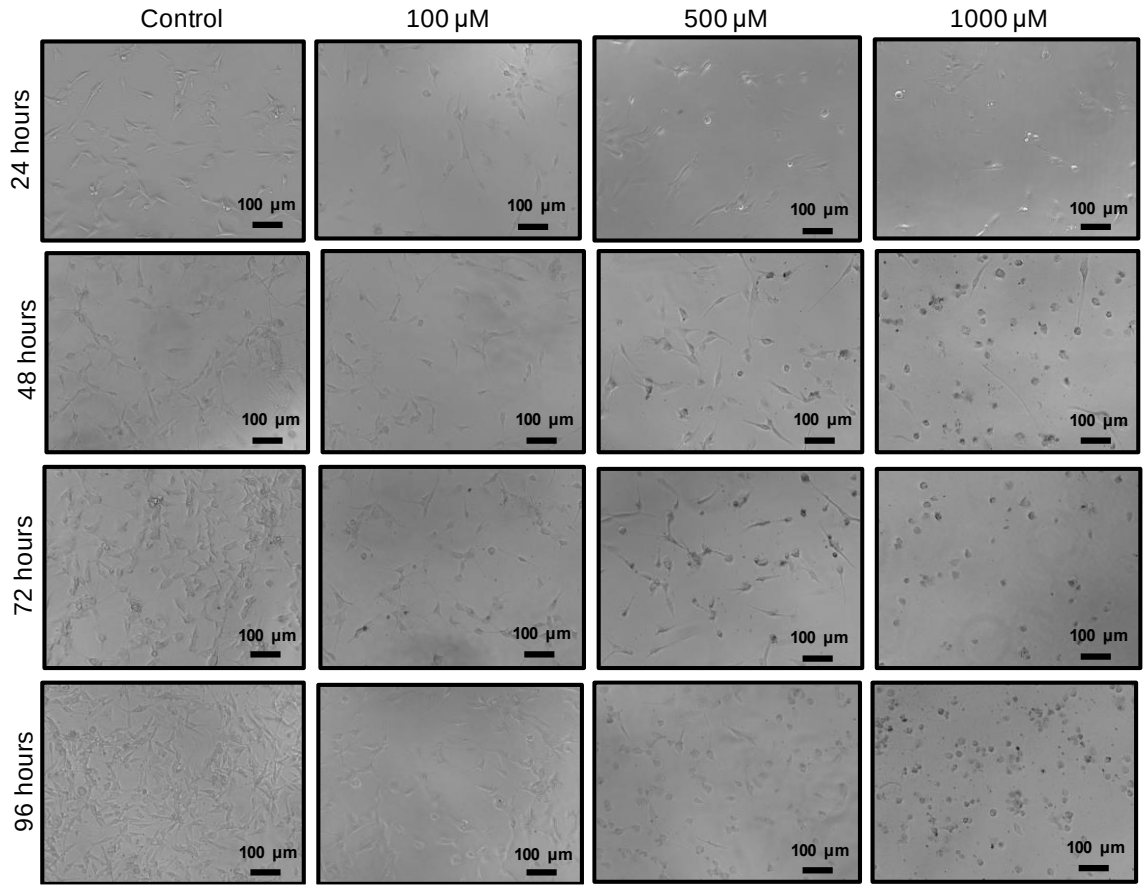

Figure 33. Microscopic images of U87 glioblastoma cells treated with different concentrations of free TMZ (100, 500, and 1000 µM) at different time points (24, 48, 72, and 96 hours).

In the case of treatment of U87 glioblastoma cells with blank meshes, cytotoxic effects were not present. However, GlioMesh demonstrated a substantial inhibition in the cell growth. A 100 µM concentration of TMZ was used for GlioMesh cell viability experiments, and the viability of U87 cells treated thus decreased considerably, 97%, after 72 hours (Figure 34). The higher cytotoxicity of GlioMesh compared with free TMZ can be attributed to the capability of GlioMesh in keeping TMZ intact within itself and releasing the drug in a sustained manner.

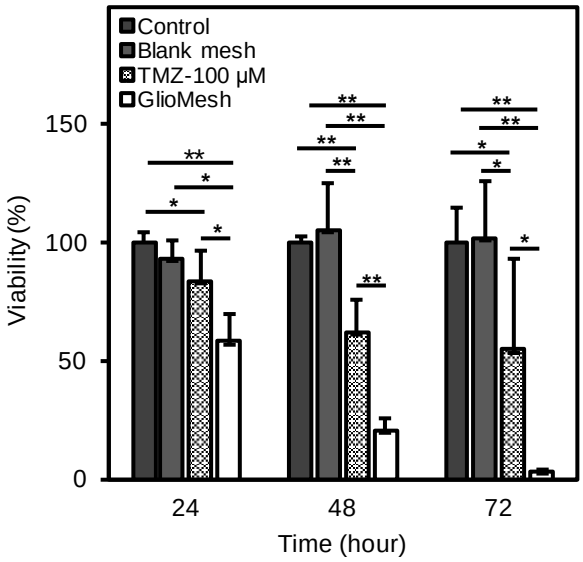

Figure 34. Cytotoxicity of blank and microsphere-loaded meshes to U87 glioblastoma cells *in vitro*. GlioMesh reduced the viability of U87 cells substantially after 72 hours of treatment. Error bars are SD (n=6). * P<0.05, and ** P<0.005.

Figure 35 shows the microscopic images of U87 glioblastoma cells after 24, 48, and 72 hours treatment with blank and microsphere-loaded meshes.

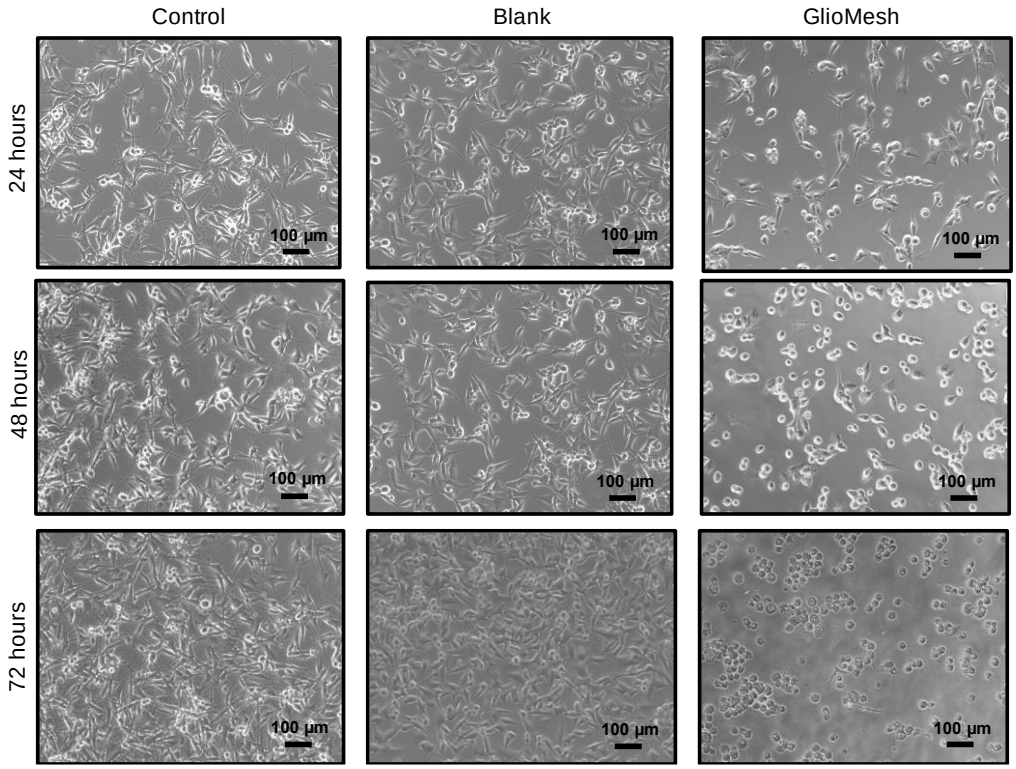

Figure 35. Microscopic images of human glioblastoma cells treated with blank and GlioMesh after 24, 48, and 72 hours.

3.3. Conclusion

Implementing a microextrusion-based 3D bioprinting technique in the fabrication of GlioMesh provides several advantages including the creation of porous 3D structures with the desired diffusive behaviour and TMZ release kinetics. This porosity also allows for the transport of oxygen and nutrients to the tissue after implantation. In addition, embedding the microspheres within the 3D bioprinted alginate mesh immobilizes the microspheres at the tumour site and prevents unwanted migration away from the desired area. GlioMesh is capable of forming a conformal contact to the irregularly shaped tissue due to the flexibility provided by alginate, the main component of bioink. This conformal contact results in utilizing the entire resection pocket which, in turn, leads to achieving high doses and homogenous distribution of TMZ. The functionality of GlioMesh regarding inducing cytotoxic effect was confirmed by conducting *in vitro* cell viability tests.

Substantially higher cytotoxicity observed for GlioMesh compared with the free drug is attributed to its sustained release properties.

Conclusion and Future Direction

Despite advances in neurosurgery, radiotherapy, and chemotherapy, the treatment of GBM, which is the most frequent and fatal adult brain tumour, remains a major challenge. Although the standard therapy for GBM patients is maximum safe surgical intervention, followed by radiotherapy plus concomitant and adjuvant chemotherapy, their prognosis is far from satisfactory. Surgeons are not usually able to remove the entire tumour mass because of topographically diffuse nature of GBM. The insensitivity of hypoxic regions of this tumour to radiotherapy adds more complications to the treatment of this aggressive disease. Additionally, the presence of BBB restricts the effective chemotherapeutics for GBM treatment. One of the most commonly used chemotherapy drugs for GBM is TMZ since it can pass the semipermeable BBB. However, there are several inadequacies associated with the systemic administration of this chemotherapeutic agent. The short half-life of TMZ necessitates high systemic administration doses. This, together with prolonged oral administration of TMZ, has numerous side effects which affect the patients' quality of life.

To tackle the shortcomings associated with traditional methods of treatment, great efforts have been made to develop new treatment methods that are capable of transporting chemotherapeutic agents efficiently across the BBB and thus decreasing the systemic toxicity. Gliadel® wafer is a commercially available localized drug delivery system approved by the US Food and Drug Administration for patients with GBM. Despite the survival benefits offered by Gliadel® wafers in the treatment of GBM, the size and rigidity of these wafers contribute to several complications for their implantation into irregularly shaped tumour tissue. Another attractive candidate that provides the advantage of

bypassing the BBB is drug-loaded polymeric microspheres. Many studies have focused on the fabrication of PLGA microspheres loaded with TMZ due to its great promise in the treatment of GBM. However, the poor encapsulation efficiency of TMZ-loaded PLGA microspheres prepared with conventional emulsion methods including o/w and w/o/w is a considerable challenge.

This thesis proposed a 3D bioprinted hydrogel-based mesh incorporated with TMZ-loaded PLGA microspheres (GlioMesh) which has the capability of releasing TMZ over a prolonged period at the tumour site. TMZ-loaded PLGA microspheres with high encapsulation efficiency were fabricated by o/o emulsion solvent evaporation method. Liquid paraffin was used as our outer phase, and high encapsulation efficiency was obtained due to the poor solubility of TMZ in the external phase. The fabricated PLGA microspheres loaded with TMZ were then embedded into an alginate mesh by using a microextrusion 3D bioprinting technique which provides several advantages. The incorporation of polymeric microspheres within the 3D bioprinted mesh allows for immobilization of microspheres at the tumour site. The porosity of 3D bioprinted structures offers the opportunity for transportation of oxygen and nutrients to the tissue after implantation. Moreover, the flexibility provided by alginate leads to a conformal contact between GlioMesh and irregular contours of brain tissue. This, in turn, results in the utilization of the entire resection cavity, thus obtaining a homogenous distribution of TMZ. Alginate fibres loaded with microspheres demonstrated a prolonged release of TMZ over 50 days. *In vitro* cell viability tests showed that the cytotoxicity of TMZ to U87 human glioblastoma cells enhanced considerably when TMZ was delivered from GlioMesh because of its sustained release manner. These results indicate that GlioMesh has excellent

potential to be used as an implant for the treatment of GBM.

As a future direction to this work, GlioMesh can be tested *in vivo* on animal models. Since the combination of other types of antitumour agents (such as paclitaxel which cannot pass the BBB) with TMZ synergistically inhibit the tumour growth, this feature can be added to GlioMesh and its functionality can be assessed. Additionally, the difference in the pH of tumour and healthy tissue can be used to make the drug delivery mechanism smarter by adding pH-responsive properties to GlioMesh.

Bibliography

Adamson, C., Kanu, O. O., Mehta, A. I., Di, C., Lin, N., Mattox, A. K., & Bigner, D. D. (2009). Glioblastoma multiforme: a review of where we have been and where we are going. *Expert Opinion on Investigational Drugs 18, No. 8, 1061–1083*.

Akbari, M., Tamayol, A., Bagherifard, S., Serex, L., Mostafalu, P., Faramarzi, N., Mohammadi, M.H. and Khademhosseini, A. (2016). Textile Technologies and Tissue Engineering: A Path Toward Organ Weaving. *Advanced Healthcare Materials*, *5*(7), 751–766. https://doi.org/10.1002/adhm.201500517

Akbari, M., Tamayol, A., Laforte, V., Annabi, N., Najafabadi, A. H., Khademhosseini, A., & Juncker, D. (2014). Composite living fibers for creating tissue constructs using textile techniques. *Advanced Functional Materials*, *24*(26), 4060–4067.

Alex, R., & Bodmeier, R. (2008). Encapsulation of water-soluble drugs by a modified solvent evaporation method. I. Effect of process and formulation variables on drug entrapment. *Journal of Microencapsulation*.

Ananta, J. S., Paulmurugan, R., Massoud, T. F., Ananta, J. S., Paulmurugan, R., & Massoud, T. F. (2016). evaluation Temozolomide-loaded PLGA nanoparticles to treat glioblastoma cells : a biophysical and cell culture evaluation. *Neurological Research*, *6412*(January 2017), 1–9. https://doi.org/10.1080/01616412.2015.1133025

Bandyopadhyay, A., Bose, S., & Das, S. (2015). 3D printing of biomaterials. *MRS Bulletin*, *40*(2), 108–114. https://doi.org/10.1557/mrs.2015.3

Black, P. (1998). Management of malignant glioma: role of surgery in relation to multimodality therapy. *Journal of Neurovirology*, *4*(2), 227–36. https://doi.org/10.3109/13550289809114522

Bodmeier, R., & McGinity, J. W. (1988). Polylactic acid microspheres containing quinidine base and quinidine sulphate prepared by the solvent evaporation method. III. Morphology of the microspheres during dissolution studies. *Journal of Microencapsulation*, *325–330*.

Cavalier, M., Benoit, J. P., & Thies, C. (1986). The formation and characterization of hydrocortisone-loaded poly ((±)-lactide) microspheres. *Journal of Pharmacy and Pharmacology*, *249–253*.

Chamberlain, M. C., & Kormanik, P. A. (1998). Practical guidelines for the treatment of malignant gliomas. *The Western Journal of Medicine*, *168*(2), 114–20. Retrieved from http://www.pubmedcentral.nih.gov/articlerender.fcgi?artid=1304839&tool=pmcentrez&rendertype=abstract

Chao, K. C., Bosch, W. R., Mutic, S., Lewis, J. S., Dehdashti, F., Mintun, M. A., Dempsey, J.F., Perez, C.A., Purdy, J.A. and Welch, M.J. (2001). A novel approach to overcome hypoxic tumor resistance: Cu-ATSM-guided intensity-modulated radiation therapy. *International Journal of Radiation Oncology• Biology• Physics 49, No. 4, 1171–1182*.

Combs, S. E., Wagner, J., Bischof, M., Welzel, T., Wagner, F., Debus, J., & Schulz-Ertner, D. (2008). Postoperative Treatment of Primary Glioblastoma Multiforme With Radiation and Concomitant Temozolomide in Elderly Patients. *International Journal of Radiation Oncology Biology Physics*, *70*(4), 987–992. https://doi.org/10.1016/j.ijrobp.2007.07.2368

Daniel, V., Brouillard, M., & Benoit, J. P. (1993). Biodegradation and brain tissue reaction

to poly (D , L-lactide-co-glycolide), *14*(6), 470–478.

DeFail, A. J., Chu, C. R., Izzo, N., & Marra, K. G. (2006). Controlled release of bioactive TGF-β1from microspheres embedded within biodegradable hydrogels. *Biomaterials*, *27*(8), 1579–1585. https://doi.org/10.1016/j.biomaterials.2005.08.013

Dilnawaz, F., & Sahoo, S. K. (2013). Enhanced accumulation of curcumin and temozolomide loaded magnetic nanoparticles executes profound cytotoxic effect in glioblastoma spheroid model. *European Journal of Pharmaceutics and Biopharmaceutics*, *85*(3 PART A), 452–462. https://doi.org/10.1016/j.ejpb.2013.07.013

Duntsch, C. (2009). Delivery of temozolomide to the tumor bed via biodegradable gel matrices in a novel model of intracranial glioma with resection, 203–212. https://doi.org/10.1007/s11060-009-9857-9

Duvvuri, S., Janoria, K. G., & Mitra, A. K. (2005). Development of a novel formulation containing poly(D,L-lactide-co- glycolide) microspheres dispersed in PLGA-PEG-PLGA gel for sustained delivery of ganciclovir. *Journal of Controlled Release*, *108*(2–3), 282–293. https://doi.org/10.1016/j.jconrel.2005.09.002

Fattal, E., De Rosa, G., & Bochot, A. (2004). Gel and solid matrix systems for the controlled delivery of drug carrier-associated nucleic acids. *International Journal of Pharmaceutics*, *277*(1–2), 25–30. https://doi.org/10.1016/j.ijpharm.2003.01.002

Flynn, J. R., Wang, L., Gillespie, D. L., Stoddard, G. J., Reid, J. K., Owens, J., Ellsworth, G.B., Salzman, K.L., Kinney, A.Y. and Jensen, R.L. (2008). Hypoxia-regulated protein expression, patient characteristics, and preoperative imaging as predictors of survival in adults with glioblastoma multiforme. *Cancer*, *113*(5), 1032–1042. https://doi.org/10.1002/cncr.23678

Fourniols, T., Randolph, L. D., Staub, A., Vanvarenberg, K., Leprince, J. G., Préat, V., des Rieux, A. and Danhier, F. (2015). Temozolomide-loaded photopolymerizable PEG-DMA-based hydrogel for the treatment of glioblastoma. *Journal of Controlled Release*, *210*, 95–104. https://doi.org/10.1016/j.jconrel.2015.05.272

Freiberg, S., & Zhu, X. X. (2004). Polymer microspheres for controlled drug release. *International Journal of Pharmaceutics*, *282*(1–2), 1–18. https://doi.org/10.1016/j.ijpharm.2004.04.013

Gao, H. (2016). Progress and perspectives on targeting nanoparticles for brain drug delivery. *Acta Pharmaceutica Sinica B*, *6*(4), 268–286. https://doi.org/10.1016/j.apsb.2016.05.013

Giaouris, E., Chorianopoulos, N., Skandamis, P. y Nychas, G. (2012). World ' s largest Science , Technology & Medicine Open Access book publisher : *Salmonella: A Dangerous Foodborne Pathogen*, 450. https://doi.org/10.5772/51895

Gil-Alegre, M. E., González-Álvarez, I., Gutiérrez-Paúls, L., & Torres-Suárez, A. I. (2008). Three weeks release BCNU loaded hydrophilic-PLGA microspheres for interstitial chemotherapy: Development and activity against human glioblastoma cells. *Journal of Microencapsulation*, *25*(8), 561–568. https://doi.org/10.1080/02652040802075799

Gökhan Eğilmez, Gürsel A. Süer,Özgüner, O. (2012). World ' s largest Science , Technology & Medicine Open Access book publisher : *Design, Control and Applications of Mechatronic Systems in Engineering*, 135–152. https://doi.org/10.5772/67458

Grizzi, I., Garreau, H., Li, S., & Vert, M. (1995). Hydrolytic degradation of devices based on poly(dl-lactic acid) size-dependence. *Biomaterials*, *16*(4), 305–311. https://doi.org/10.1016/0142-9612(95)93258-F

Guerin, C., Olivi, A., Weingart, J. D., Lawson, H. C., & Brem, H. (2004). Recent advances in brain tumor therapy: Local intracerebral drug delivery by polymers. *Investigational New Drugs*, *22*(1), 27–37. https://doi.org/10.1023/B:DRUG.0000006172.65135.3e

Gutman, R. L., Peacock, G., & Lu, D. R. (2000). Targeted drug delivery for brain cancer treatment. *Journal of Controlled Release*, *65*(1–2), 31–41. https://doi.org/10.1016/S0168-3659(99)00229-1

Hou, L. C., Veeravagu, A., Hsu, A. R., & Tse, V. C. K. (2006). Recurrent glioblastoma multiforme: a review of natural history and management options. *Neurosurgical Focus*, *20*(4), E3. https://doi.org/10.3171/foc.2006.20.4.2

Iqbal, M., Zafar, N., Fessi, H., & Elaissari, A. (2015). Double emulsion solvent evaporation techniques used for drug encapsulation, *496*, 173–190.

Jawhari, S., Ratinaud, M. H., & Verdier, M. (2016). Glioblastoma, hypoxia and autophagy: A survival-prone "ménage-à-trois." *Cell Death and Disease*, *7*(10), 1–10. https://doi.org/10.1038/cddis.2016.318

Juillerat-Jeanneret, L. (2008). The targeted delivery of cancer drugs across the blood-brain barrier: chemical modifications of drugs or drug-nanoparticles? *Drug Discovery Today*, *13*(23–24), 1099–1106. https://doi.org/10.1016/j.drudis.2008.09.005

Juillerat-Jeanneret, L., & Schmitt, F. (2007). Chemical modification of therapeutic drugs or drug vector systems to achieve targeted therapy: Looking for the grail. *Medicinal Research Reviews*, *27*(4), 574–590. https://doi.org/10.1002/med.20086

Kalaskar, D. (Ed.). (2017). *3D Printing in Medicine*. Woodhead Publishing.

Kashi, T. S. J., Eskandarion, S., Esfandyari-Manesh, M., Marashi, S. M. A., Samadi, N., Fatemi, S. M., Atyabi, F., Eshraghi, S. and Dinarvand, R. (2012). Improved drug loading and antibacterial activity of minocycline-loaded PLGA nanoparticles prepared by solid / oil / water ion pairing method. *International Journal of Nanomedicine*, *7*, 221–234. https://doi.org/Doi 10.2147/Ijn.S27709

Kennedy, J. P., & Curtis, E. J. I. (2002). Semisolid therapeutic delivery system and combination semisolid, multiparticulate, therapeutic delivery system. *U.S. Patent 6,488,952*.

Kreuter, J., Shamenkov, D., Petrov, V., Ramge, P., Cychutek, K., Koch-Brandt, C., & Alyautdin, R. (2002). Apolipoprotein-mediated transport of nanoparticle-bound drugs across the blood-brain barrier. *Journal of Drug Targeting*, *10*(4), 317–325. https://doi.org/10.1080/10611860290031877

Lee, J., & Lee, K. Y. (2009). Injectable microsphere/hydrogel combination systems for localized protein delivery. *Macromolecular Bioscience*, *9*(7), 671–676. https://doi.org/10.1002/mabi.200800317

Lee, K. Y., & Yuk, S. H. (2007). Polymeric protein delivery systems. *Progress in Polymer Science (Oxford)*, *32*(7), 669–697. https://doi.org/10.1016/j.progpolymsci.2007.04.001

Lesniak, M. S., & Brem, H. (2004). Targeted therapy for brain tumours. *Nature Reviews Drug Discovery*, *3*(6), 499–508. https://doi.org/10.1038/nrd1414

Lockman, P. R., Mumper, R. J., Khan, M. A., & Allen, D. D. (2002). Nanoparticle technology for drug delivery across the blood-brain barrier. *Drug Development and*

Industrial Pharmacy, *28*(1), 1–13. https://doi.org/10.1081/DDC-120001481

Luo, Y., Lode, A., & Gelinsky, M. (2013). Direct Plotting of Three-Dimensional Hollow Fiber Scaffolds Based on Concentrated Alginate Pastes for Tissue Engineering. *Advanced Healthcare Materials*, *2*(6), 777–783. https://doi.org/10.1002/adhm.201200303

Mahdavi, H., Mirzadeh, H., Hamishehkar, H., Jamshidi, A., Fakhari, A., Emami, J., & Najafabadi, A. R. (2010). The effect of process parameters on the size and morphology of poly (D, L-lactide-co-glycolide) micro/nanoparticles prepared by an oil in oil emulsion/solvent evaporation technique. *Journal of Applied Polymer Science 116, No. 1, 528–534*.

Mehta, A. M., Sonabend, A. M., & Bruce, J. N. (2017). Convection-Enhanced Delivery. *Neurotherapeutics*, *14*(2), 358–371. https://doi.org/10.1007/s13311-017-0520-4

Michaelis, K. (2006). Covalent Linkage of Apolipoprotein E to Albumin Nanoparticles Strongly Enhances Drug Transport into the Brain. *Journal of Pharmacology and Experimental Therapeutics*, *317*(3), 1246–1253. https://doi.org/10.1124/jpet.105.097139

Murphy, S. V, & Atala, A. (2014). 3D bioprinting of tissues and organs. *Nature Biotechnology*, *32*(8), 773–785. https://doi.org/10.1038/nbt.2958

Newlands, E. S., Stevens, M. F. G., Wedge, S. R., Wheelhouse, R. T., & Brock, C. (1997). Temozolomide: A review of its discovery, chemical properties, pre-clinical development and clinical trials. *Cancer Treatment Reviews*, *23*(1), 35–61. https://doi.org/10.1016/S0305-7372(97)90019-0

O'Donnell, P. B., & McGinity, J. W. (1997). Preparation of microspheres by the solvent evaporation technique. *Advanced Drug Delivery Reviews*, *28*(1), 25–42. https://doi.org/10.1016/S0169-409X(97)00049-5

Ohgaki, H., & Kleihues, P. (2007). Genetic Pathways to Primary and Secondary Glioblastoma. *The American Journal of Pathology*, *170*(5), 1445–1453. https://doi.org/10.2353/ajpath.2007.070011

Omuro, A., & DeAngelis, L. M. (2013). Glioblastoma and other malignant gliomas: A clinical review. *JAMA - Journal of the American Medical Association*, *310*(17), 1842–1850. https://doi.org/10.1001/jama.2013.280319

Pedde, R. D., Mirani, B., Navaei, A., Styan, T., Wong, S., & Mehrali, M. (2017). Emerging Biofabrication Strategies for Engineering Complex Tissue Constructs Emerging Biofabrication Strategies for Engineering Complex Tissue Constructs, (July). https://doi.org/10.1002/adma.201606061

Pourgholi, F., & Farhad, J. (2016). ScienceDirect Nanoparticles : Novel vehicles in treatment of Glioblastoma, *77*, 98–107. https://doi.org/10.1016/j.biopha.2015.12.014

Pourgholi, F., hajivalili, M., Farhad, J. N., Kafil, H. S., & Yousefi, M. (2016). Nanoparticles: Novel vehicles in treatment of Glioblastoma. *Biomedicine and Pharmacotherapy*, *77*, 98–107. https://doi.org/10.1016/j.biopha.2015.12.014

Rottenberg, D. A., Ginos, J. Z., Kearfott, K. J., Junck, L., Dhawan, V., & Jarden, J. (1985). In Vivo Measurement of Brain Tumor pH Using {" C } DMO and Positron Emission Tomography, 70–79.

Salvati, A., Pitek, A. S., Monopoli, M. P., Prapainop, K., Bombelli, F. B., Hristov, D. R., Kelly, P.M., Åberg, C., Mahon, E. and Dawson, K.A. (2013). Transferrin-functionalized nanoparticles lose their targeting capabilities when a biomolecule

corona adsorbs on the surface. *Nature Nanotechnology*, *8*(2), 137–143. https://doi.org/10.1038/nnano.2012.237

Smith, A. (1986). Evaluation of poly (lactic acid) as a biodegradable drug delivery system for parenteral administration. *International Journal of Pharmaceutics*, *215–220*.

Steiniger, S. C. J., Kreuter, J., Khalansky, A. S., Skidan, I. N., Bobruskin, A. I., Smirnova, Z. S., Severin, S.E., Uhl, R., Kock, M., Geiger, K.D. and Gelperina, S.E. (2004). Chemotherapy of glioblastoma in rats using doxorubicin-loaded nanoparticles. *International Journal of Cancer*, *109*(5), 759–767. https://doi.org/10.1002/ijc.20048

Stewart, L. A. (2002). Chemotherapy in adult high-grade glioma: A systematic review and meta-analysis of individual patient data from 12 randomised trials. *Lancet*, *359*(9311), 1011–1018. https://doi.org/10.1016/S0140-6736(02)08091-1

Stupp, R., Mason, W. P., van den Bent, M. J., Weller, M., Fisher, B., Taphoorn, M. J. B., Belanger, K., Brandes, A.A., Marosi, C., Bogdahn, U. and Curschmann, J. (2005). Radiotherapy plus Concomitant and Adjuvant Temozolomide for Glioblastoma. *New England Journal of Medicine*, *352*(10), 987–996. https://doi.org/10.1056/NEJMoa043330

Suzuki, K., & Price, J. C. (1985). Microencapsulation and dissolution properties of a neuroleptic in a biodegradable polymer, poly (d, l-lactide). *Journal of Pharmaceutical Sciences*, *21–24*.

Tamayol, A., Akbari, M., Annabi, N., Paul, A., Khademhosseini, A., & Juncker, D. (2013). Fiber-based tissue engineering: Progress, challenges, and opportunities. *Biotechnology Advances*, *31*(5), 669–687. https://doi.org/10.1016/j.biotechadv.2012.11.007

Thakkar, J. P., Dolecek, T. A., Horbinski, C., Ostrom, Q. T., Lightner, D. D., Barnholtz-Sloan, J. S., & Villano, J. L. (2014). Epidemiologic and molecular prognostic review of glioblastoma. *Cancer Epidemiology Biomarkers and Prevention*, *23*(10), 1985–1996. https://doi.org/10.1158/1055-9965.EPI-14-0275

Uchegbu, I. F., & Schatzlein, A. G. (Eds.). (2006). *Polymers in drug delivery*. CRC Press.

Ungaro, F., Biondi, M., d'Angelo, I., Indolfi, L., Quaglia, F., Netti, P. A., & La Rotonda, M. I. (2006). Microsphere-integrated collagen scaffolds for tissue engineering: Effect of microsphere formulation and scaffold properties on protein release kinetics. *Journal of Controlled Release*, *113*(2), 128–136. https://doi.org/10.1016/j.jconrel.2006.04.011

Vert, M., Mauduit, J., & Li, S. (1994). Biodegradation of PLA / GA polymers : increasing complexity. *Biomaterials*, *15*(15), 1209–1213. https://doi.org/http://dx.doi.org/10.1016/0142-9612(94)90271-2

Wakiyama, N., JUNI, K., & NAKANO, M. (1982). Preparation and evaluation in vitro and in vivo of polylactic acid microspheres containing dibucaine. *Chemical and Pharmaceutical Bulletin*, *3719–3727*.

Westphal, M., Ram, Z., Riddle, V., Hilt, D., & Bortey, E. (2006). Gliadel® wafer in initial surgery for malignant glioma: Long-term follow-up of a multicenter controlled trial. *Acta Neurochirurgica*, *148*(3), 269–275. https://doi.org/10.1007/s00701-005-0707-z

Wheelhouse, R. T., & Stevens, M. F. G. (1993). ID +, (15), 1177–1178.

White, E., Bienemann, A., Malone, J., Megraw, L., Bunnun, C., Wyatt, M., & Gill, S. (2011). An evaluation of the relationships between catheter design and tissue mechanics in achieving high-flow convection-enhanced delivery. *Journal of*

Neuroscience Methods, *199*(1), 87–97. https://doi.org/10.1016/j.jneumeth.2011.04.027

Wilson, T. A., Karajannis, M. A., & Harter, D. H. (2014). Glioblastoma multiforme: State of the art and future therapeutics. *Surgical Neurology International*, *5*, 64. https://doi.org/10.4103/2152-7806.132138

Wohlfart, S., Gelperina, S., & Kreuter, J. (2012). Transport of drugs across the blood-brain barrier by nanoparticles. *Journal of Controlled Release*, *161*(2), 264–273. https://doi.org/10.1016/j.jconrel.2011.08.017

Woodworth, G. F., Dunn, G. P., Nance, E. A., Hanes, J., & Brem, H. (2014). Emerging Insights into Barriers to Effective Brain Tumor Therapeutics. *Frontiers in Oncology*, *4*(July), 1–14. https://doi.org/10.3389/fonc.2014.00126

Wu, L., & Ding, J. (2004). In vitro degradation of three-dimensional porous poly(d,l-lactide-co-glycolide) scaffolds for tissue engineering. *Biomaterials*, *25*(27), 5821–5830. https://doi.org/10.1016/j.biomaterials.2004.01.038

Yeo, Y., & Park, K. (2004). Control of Encapsulation Efficiency and Initial Burst in Polymeric Microparticle Systems, *27*(1), 1–12.

Yong, K., & Mooney, D. J. (2012). Progress in Polymer Science Alginate : Properties and biomedical applications. *Progress in Polymer Science*, *37*(1), 106–126. https://doi.org/10.1016/j.progpolymsci.2011.06.003

Zhang, H., & Gao, S. (2007). Temozolomide / PLGA microparticles and antitumor activity against Glioma C6 cancer cells in vitro, *329*, 122–128. https://doi.org/10.1016/j.ijpharm.2006.08.027

Zhang, J., Stevens, M. F. G., & Bradshaw, T. D. (2012). Temozolomide : Mechanisms of Action , Repair and Resistance, 102–114.

Zolnik, B. S., & Burgess, D. J. (2007). Effect of acidic pH on PLGA microsphere degradation and release. *Journal of Controlled Release*, *122*(3), 338–344. https://doi.org/10.1016/j.jconrel.2007.05.034

Zolnik, B. S., Leary, P. E., & Burgess, D. J. (2006). Elevated temperature accelerated release testing of PLGA microspheres. *Journal of Controlled Release*, *112*(3), 293–300. https://doi.org/10.1016/j.jconrel.2006.02.015

Zvi, L., Maedor, Y., Jonas, T., Pfeffer, R., Faibel, M., Nass, D., Hadani, M. and Ram, Z. (2004). Convection-enhanced delivery of paclitaxel for the treatment of recurrent malignant glioma: a phase I/II clinical study. *Journal of Neurosurgery*, *472–479*.